

Effect of TiO_2 polymorphs and crystallite size on the catalytic properties of Pt/ TiO_2 in the
selective hydrogenation of furfural to furfuryl alcohol



A Thesis Submitted in Partial Fulfillment of the Requirements
for the Degree of Master of Engineering in Chemical Engineering

Department of Chemical Engineering

Faculty of Engineering

Chulalongkorn University

Academic Year 2018

Copyright of Chulalongkorn University

ผลของโครงสร้างและขนาดผลึกไทเทเนียมไดออกไซด์ต่อสมบัติในการทำปฏิกิริยาของ Pt/TiO_2 ใน
ปฏิกิริยาไฮโดรจีเนชันแบบเจาะจงของเฟอร์ฟูรัลเป็นเฟอร์ฟิวรีลแอลกอฮอล์



วิทยานิพนธ์นี้เป็นส่วนหนึ่งของการศึกษาตามหลักสูตรปริญญาวิศวกรรมศาสตรมหาบัณฑิต

สาขาวิชาวิศวกรรมเคมี ภาควิชาวิศวกรรมเคมี

คณะวิศวกรรมศาสตร์ จุฬาลงกรณ์มหาวิทยาลัย

ปีการศึกษา 2561

ลิขสิทธิ์ของจุฬาลงกรณ์มหาวิทยาลัย

Thesis Title Effect of TiO₂ polymorphs and crystallite size on the
 catalytic properties of Pt/TiO₂ in the selective
 hydrogenation of furfural to furfuryl alcohol

By Miss Thunyakorn Kaewla-ueat

Field of Study Chemical Engineering

Thesis Advisor Professor JOONGJAI PANPRANOT, Ph.D.

Accepted by the Faculty of Engineering, Chulalongkorn University in Partial
Fulfillment of the Requirement for the Master of Engineering

..... Dean of the Faculty of Engineering
(Professor SUPOT TEACHAVORASINSKUN, D.Eng.)

THESIS COMMITTEE

..... Chairman
(Assistant Professor PALANG BUMROONGSAKULSAWAT,
Ph.D.)

..... Thesis Advisor
(Professor JOONGJAI PANPRANOT, Ph.D.)

..... Examiner
(Associate Professor DEACHA CHATSIRIWECH, Ph.D.)

..... External Examiner
(Assistant Professor Okorn Mekasuwandumrong, D.Eng.)

ธัญพร แก้วละเอียด : ผลของโครงสร้างและขนาดผลึกไทเทเนียมไดออกไซด์ต่อสมบัติในการทำปฏิกิริยาของ Pt/TiO₂ ในปฏิกิริยาไฮโดรจิเนชันแบบเจาะจงของเฟอร์ฟูรัลเป็นเฟอร์ฟิวรัลแอลกอฮอล์. (Effect of TiO₂ polymorphs and crystallite size on the catalytic properties of Pt/TiO₂ in the selective hydrogenation of furfural to furfuryl alcohol) อ.ที่ปรึกษาหลัก : ศ. ดร.จูงใจ ปั้นประณต

เฟอร์ฟิวรัลแอลกอฮอล์เป็นสารมัธยันตร์ที่มีความสำคัญต่อการผลิตสารเคมีมูลค่าสูงหลายชนิด อาทิ ฟิวรีน เรซิน วิตามิน C และไลซีน ซึ่งในงานวิจัยนี้ปฏิกิริยาไฮโดรจิเนชันแบบเจาะจงของเฟอร์ฟูรัลเป็นเฟอร์ฟิวรัลแอลกอฮอล์ดำเนินการที่อุณหภูมิ 50 องศาเซลเซียส ความดันไฮโดรเจน 20 บาร์ และเวลาในการทำปฏิกิริยา 2 ชั่วโมง โดยใช้ตัวเร่งปฏิกิริยาแพลทินัมบนตัวรองรับไทเทเนียมไดออกไซด์ที่มี 0.5 เปอร์เซ็นต์โดยน้ำหนักของแพลทินัม ตัวเร่งปฏิกิริยาถูกเตรียมด้วยวิธีเคลือบฝังโดยตัวรองรับไทเทเนียมไดออกไซด์ทางการค้าที่มีโครงสร้างต่างกันและตัวรองรับไทเทเนียมไดออกไซด์ไซลเจลที่เผาในอุณหภูมิที่ต่างกัน พบว่าในกลุ่มของไทเทเนียมไดออกไซด์ทางการค้า ตัวรองรับไทเทเนียมไดออกไซด์ชนิด P25 ให้ค่าการเปลี่ยนแปลงของเฟอร์ฟูรัลและค่าการเลือกเกิดเป็นเฟอร์ฟิวรัลแอลกอฮอล์ที่ดีที่สุด ที่ 81 เปอร์เซ็นต์ และ 98 เปอร์เซ็นต์ตามลำดับ และการใช้ตัวรองรับไทเทเนียมไดออกไซด์ที่เตรียมเองโดยวิธีไซลเจลที่เผาในอุณหภูมิ 600 องศาเซลเซียส ให้ค่าการเปลี่ยนแปลงของเฟอร์ฟูรัลและค่าการเลือกเกิดเป็นเฟอร์ฟิวรัลแอลกอฮอล์ที่ดีที่สุด ที่ 88 เปอร์เซ็นต์ และ 93 เปอร์เซ็นต์ตามลำดับ คาดว่าการใช้ไทเทเนียมไดออกไซด์ที่มีโครงสร้างแบบผสมสามารถเพิ่มประสิทธิภาพของตัวเร่งปฏิกิริยา ซึ่งสอดคล้องกับผลการวิเคราะห์คุณลักษณะของตัวเร่งปฏิกิริยาด้วยเทคนิคการวัดกัมมันตภาพรังสีของไฮโดรเจนด้วยการโปรแกรมอุณหภูมิ เอ็กซ์เรย์โฟโตอิเล็กตรอนสเปกโตรสโกปี และกล้องจุลทรรศน์อิเล็กตรอนแบบส่องผ่าน นอกจากนี้แพลทินัมยังแสดงการไฮโดรจิเนชันแบบเจาะจงของเฟอร์ฟูรัลเป็นเฟอร์ฟิวรัลแอลกอฮอล์

สาขาวิชา	วิศวกรรมเคมี	ลายมือชื่อนิสิต
	
ปี	2561	ลายมือชื่อ อ.ที่ปรึกษาหลัก
การศึกษา	

ACKNOWLEDGEMENTS

First, I would like to express my sincere and thanks for to my thesis advisor, Professor Joongjai Panpranot of for her valuable suggestions, motivation, encouragement and made my thesis completed. This thesis would not have been completed if without her support.

Moreover, I would like to acknowledge Assistant Professor Dr. Palang Bumroongsakulsawat of the Department of Chemical Engineering at Chulalongkorn University as my thesis chairman, Associate Professor Dr. Deacha Chatsiriwech of the Department of Chemical Engineering at Chulalongkorn University and Assistant Professor Dr. Okorn Mekasuwandumrong of the Department of Chemical Engineering, Faculty Of Engineering And Industrial Technology, Silpakorn University as the members of my thesis committee.

Finally, I gratefully thank my family and my friends for providing me for continuous support and encouragement throughout my study year and through the period of this research.



จุฬาลงกรณ์มหาวิทยาลัย
CHULALONGKORN UNIVERSITY

Thunyaporn Kaewla-ueat

TABLE OF CONTENTS

	Page
ABSTRACT (THAI).....	iii
ABSTRACT (ENGLISH)	iv
ACKNOWLEDGEMENTS.....	v
TABLE OF CONTENTS.....	vi
LIST OF TABLES.....	ix
LIST OF FIGURES	x
CHAPTER I INTRODUCTION.....	1
1.1 Introduction	1
1.2 Objectives of the Research	3
1.3 Scope of the Research	3
1.4 Research Methodology.....	4
CHAPTER II BACKGROUND AND LITERATURE REVIEW	5
2.1 Hydrogenation Reactions	5
2.2 Properties of Platinum	5
2.3 TiO ₂ support	6
2.4 Sol-gel	7
2.5 Strong metal-support interaction (SMSI)	8
2.6 Hydrogenation of furfural to furfuryl alcohol	8
2.7 Effect of TiO ₂ support on hydrogenation reaction	19
2.8 The effect of calcination temperature on the sol-gel synthesized TiO ₂ support.....	21
CHAPTER III MATERIALS AND METHODS	25

3.1 Catalyst preparation.....	25
3.1.1 Preparation of TiO ₂ supported Pt catalysts.....	25
3.1.2 Preparation of TiO ₂ sol-gel support.....	26
3.1.3 Preparation of TiO ₂ sol-gel support Pt catalysts	27
3.2 Catalytic test in the selective hydrogenation of furfural	27
3.3 Catalyst Characterization.....	29
3.3.1 X-ray photoelectron spectroscopy (XPS).....	29
3.3.2 X-ray diffraction (XRD).....	29
3.3.3 N ₂ -physisorption	30
3.3.4 Hydrogen Temperature-programmed reduction (H ₂ -TPR)	30
3.3.5 CO pulse chemisorption.....	30
3.3.6 Transmission electron spectroscopy (TEM)	30
CHAPTER IV	31
RESULTS AND DISCUSSION	31
4.1 The characterization of Pt/TiO ₂ with different TiO ₂ polymorphs.....	31
4.1.1 X-ray diffraction (XRD).....	31
4.1.2 CO pulse Chemisorption	33
4.1.3 N ₂ Physisorption	34
4.1.4 The H ₂ -temperature programmed reduction (H ₂ -TPR)	37
4.1.5 Transmission electron spectroscopy (TEM)	38
4.1.6 X-ray photoelectron spectroscopy (XPS).....	39
4.2 Evaluation of the catalyst performance in the selective furfural hydrogenation	43

4.3 The characterization of Pt/TiO ₂ sol-gel with different calcination temperatures of the TiO ₂	45
4.3.1 X-ray diffraction (XRD).....	45
4.3.2 N ₂ -physisorption	47
4.3.3 The H ₂ -temperature programmed reduction (H ₂ -TPR)	48
4.3.4 Transmission electron spectroscopy (TEM)	49
4.3.5 X-ray photoelectron spectroscopy (XPS)	50
4.4 The catalytic performance of Pt/TiO ₂ with different temperature calcined TiO ₂	52
CHAPTER V	53
CONCLUSIONS AND RECOMMENDATION	53
5.1 Conclusions.....	53
5.2 Recommendations	53
REFERENCES.....	54
VITA	69

LIST OF TABLES

	Page
Table 1 Physical properties of Platinum.....	6
Table 2 Summary of the research of the furfural hydrogenation on various catalysts under different reaction condition.	10
Table 3 Summary of the research on the effect of TiO ₂ structure support for the hydrogenation reaction	19
Table 4 Summary of the research on the effect of calcination temperature on the sol-gel synthesized TiO ₂	21
Table 5 Chemicals used for catalyst preparation (incipient impregnation method)	25
Table 6 Support used for catalyst preparation (incipient impregnation method)	25
Table 7 Chemical used for TiO ₂ preparation by sol-gel method	27
Table 8 Chemicals used in the liquid-phase furfural hydrogenation.....	28
Table 9 Gas-Chromatography operating conditions	28
Table 10 Pt/TiO ₂ prepared with different TiO ₂ polymorphs consisting of various % anatase of TiO ₂	32
Table 11 CO chemisorption results of Pt/TiO ₂ with different TiO ₂ polymorphs.....	33
Table 12 BET surface area, pore volume, pore diameter and average pore diameter of the catalysts.....	35
Table 13 Reaction results of the Pt/TiO ₂ catalysts.	44
Table 14 The amount of Pt loading in TiO ₂	45

LIST OF FIGURES

	Page
Figure 1 TiO ₂ crystal structures: rutile (a), anatase (b) and brookite (c)	7
Figure 2 Simplified reaction scheme of the hydrogenation of furfural.....	9
Figure 3 Application of furfuryl alcohol	9
Figure 4 The XRD patterns of TiO ₂ nanoparticle.....	24
Figure 5 Diagram of Pt on TiO ₂ catalysts preparation by incipient wetness impregnation method.....	26
Figure 6 Diagram of TiO ₂ catalyst preparation by sol-gel method	27
Figure 7 Schematic of the liquid-phase hydrogenation of furfural.	29
Figure 8 The XRD pattern of Pt/TiO ₂ catalysts prepared with different TiO ₂ polymorphs.	32
Figure 9 N ₂ -Physisorption isotherms of Pt/P25, Pt/A1, Pt/A2, Pt/R1, and Pt/R2	36
Figure 10 The combination of N ₂ -Physisorption isotherms of Pt/P25, Pt/A1, Pt/A2, Pt/R1, and Pt/R2	36
Figure 11 The H ₂ -TPR profiles of Pt/P25, Pt/A1, Pt/A2, Pt/R1, and Pt/R2	37
Figure 12 The TEM of Pt/P25, Pt/A1, Pt/A2, Pt/R1 and Pt/R2	39
Figure 13 XPS spectra of Ti 2p of bare TiO ₂ support	41
Figure 14 XPS spectra of Ti 2p of Pt/P25, Pt/A1, Pt/A2, Pt/R1 and Pt/R2.....	41
Figure 15 XPS spectra of O 1s of TiO ₂ support	42
Figure 16 XPS spectra of O 1s of Pt/P25, Pt/A1, Pt/A2, Pt/R1 and Pt/R2	42
Figure 17 The pathway of furfural hydrogenation	43
Figure 18 The XRD patterns of Pt/TiO ₂ catalysts with different temperature calcined TiO ₂	46

Figure 19 N ₂ -Physisorption isotherms of Pt/TiO ₂ with different temperature calcined TiO ₂	48
Figure 20 The H ₂ -TPR profiles of Pt/TiO ₂ with different temperature calcined TiO ₂	49
Figure 21 The TEM of Pt/TiO ₂ with different temperature calcined TiO ₂	50
Figure 22 XPS spectra of Ti 2p of Pt/TiO ₂ with different temperature calcined TiO ₂	51
Figure 23 XPS spectra of O 1s of Pt/TiO ₂ with different temperature calcined TiO ₂	51



CHAPTER I

INTRODUCTION

1.1 Introduction

The production of most chemical products has been relied on fossil fuels as feedstock, but they are non-renewable and caused global warming. Therefore, renewable biomass has received considerable attention to replace fossil fuels because biomass can convert to many chemicals such as cellulose, vanillin, and furfural. Furfural is an aldehyde of furan. It is a biomass-derived chemical, produced by acid-catalyzed dehydration of xylose, the main building-block of hemicellulose constituent of lignocellulose [1]. The hydrogenation of furfural has many pathways to produce many products such as furfuryl alcohol, furan, 2-methylfuran, 2-methyl tetrahydrofuran, and tetrahydrofurfuryl alcohol. Furfuryl alcohol (FA) is the main product from the selective hydrogenation of furfural [2]. FA is an interesting high value chemical and important chemical intermediate for the production of chemical products in wide applications, such as vitamin C, lysine, plasticizer, dispersing agent, lubricant and resin[3].

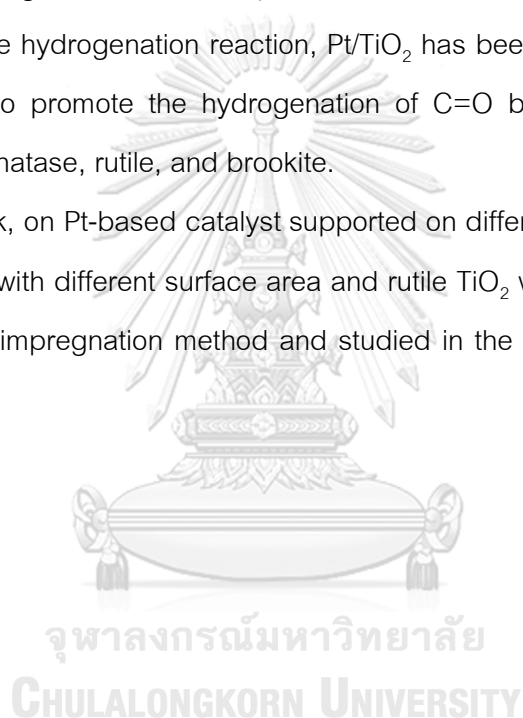
Furfural contains two function groups C=C double bond and C=O double bond, which can be hydrogenated. To produce FA, furfural is hydrogenated at C=O bond to get FA[4]. Cu-Cr based catalysts are used in industry to produce furfuryl alcohol under conditions approximately 180°C and 70-100 bar pressure but it is found to be toxic due to the presence of Cr₂O₃ and can have an impact on the environmental pollution and toxicity[1]. Noble metals have been considered as alternatives catalysts instead of Cu-Cr based catalysts because noble metals such as Pt and Pd based catalysts did not have much effect on the environment and have been investigated for catalytic hydrogenation of furfural to produce FA in liquid phase hydrogenation[3]. Platinum(Pt) catalysts are known to be effective for furfural hydrogenation because they facilitate the partial hydrogenation furfural to FA by C=O hydrogenation[5].

Bimetallic catalysts are also interesting in hydrogenation reaction because the addition of a second metal can improve the conversion and selectivity. Nickel (Ni) is an

interesting promoter for platinum catalysts. For example, Liu, L. et al.(2017) [5] reported that Pd-Ni/MWNT showed enhance the catalytic activity for furfural hydrogenation in liquid phase and can hydrogenate for both C=C and C=O group forming THFA, that has wide application in preparation of 1-5-pentadiols, printing inks, agricultural application, and electronics cleaners.

Titanium dioxide (TiO_2) is used as catalyst support in many reactions such as hydrogenation, dehydrogenation, and photocatalyst due to, its nontoxicity and high effectiveness. At high reduction temperature, it shows the strong metal support interaction[6]. In the hydrogenation reaction, Pt/ TiO_2 has been used a catalyst and, TiO_2 has been shown to promote the hydrogenation of C=O bond[7]. TiO_2 exists in three crystalline forms; anatase, rutile, and brookite.

In this work, on Pt-based catalyst supported on different TiO_2 polymorphs (P-25, pure anatase TiO_2 with different surface area and rutile TiO_2 with different surface areas) were prepared by impregnation method and studied in the hydrogenation of furfural to furfuryl alcohol.



1.2 Objectives of the Research

To study the characteristics and catalytic properties of TiO₂ supported Pt nanoparticles prepared with P-25, pure anatase TiO₂, rutile TiO₂, and sol-gel derived TiO₂ in the liquid phase selective furfural hydrogenation.

1.3 Scope of the Research

1.3.1 Preparation of Pt/TiO₂ catalysts by impregnation with Pt content 0.5 wt% support with different TiO₂ polymorphs (P-25, pure anatase TiO₂ with different surface area and rutile TiO₂ with different surface area) were prepared by using incipient wetness impregnation method and calcined at 400°C under air atmospheres for 4 h.

1.3.2 The TiO₂ support were prepared using the sol-gel method and various temperature calcination at 400, 500, 600, and 700°C under air atmospheres for 4 h.

1.3.3 Preparation of Pt/TiO₂ catalysts Pt content 0.5 wt% support with different temperature calcined TiO₂ were prepared by using incipient wetness impregnation method and calcined at 400, 500, 600, and 700°C under air atmospheres for 4 h.

1.3.4 The reduction conditions were H₂ flow (25cm³/min) at 500°C for 2h.

1.3.5 The catalysts were tested in the hydrogenation of furfural in a batch reactor at constant temperature 50°C and pressure 20 bars in hydrogen for 2 h using methanol as a solvent.

1.3.6 Characterization of the prepared catalysts by various method including

1.3.2.1 N₂ physisorption

1.3.2.2 X-ray diffraction (XRD)

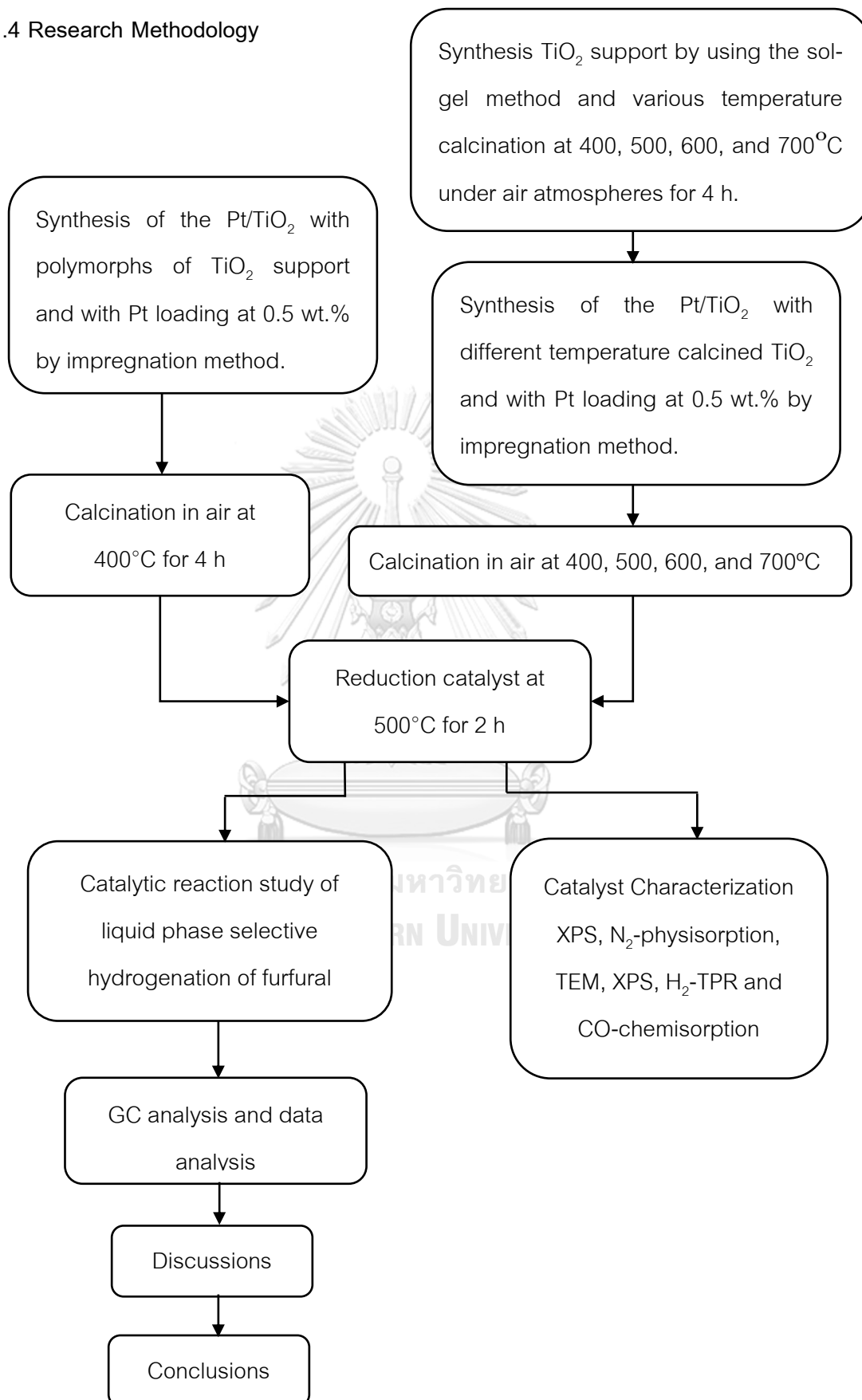
1.3.2.3 CO pulse chemisorption

1.3.2.4 H₂-temperature programmed reduction (H₂-TRR)

1.3.2.5 Transmission electron spectroscopy (TEM)

1.3.2.6 X-ray photoelectron spectroscopy (XPS)

1.4 Research Methodology



CHAPTER II

BACKGROUND AND LITERATURE REVIEW

2.1 Hydrogenation Reactions

Hydrogenation is a chemical reaction which treatment of substances with molecular hydrogen (H_2) occurs by adding pairs of hydrogen atom to compound (generally unsaturated compound). This process is useful in wide industrial such as food industry, petrochemical industry, and agricultural industry [8, 9].

Hydrogenation reactions will not occur between hydrogen and organic compound below $480^\circ C$ without metal catalysts. These usually require a catalyst for the reaction to occur under normal conditions of temperature and pressure. Hydrogenation reactions generally require three components: the substrate, the hydrogen source, and a catalyst. Catalysts are responsible for binding the H_2 molecule and facilitating the reaction between the hydrogen and the substrate. Platinum, palladium, rhodium, and ruthenium [10] are active catalysts which can operate at lower temperatures and pressure [11].

Heterogeneous catalysts are commonly used in hydrogenation reactions because reactant and catalyst are in different phases, they can be easily separated from a product. On the other hand, homogeneous catalysts, catalysts are in the same phase as the reactants because the catalyst is dissolved in reactant [12].

2.2 Properties of Platinum

Platinum is a chemical element with chemical symbol Pt and an atomic number of 78 (Table 1). Platinum is in group 10 of the periodic table of elements. Platinum is a dense, malleable, ductile, precious, gray-white transition metal, resistant to corrosion [13]. Platinum has six naturally isotopes: ^{190}Pt , ^{192}Pt , ^{194}Pt , ^{195}Pt , ^{196}Pt , and ^{198}Pt [14]. The most abundant of these is ^{195}Pt . The applications of platinum have used in many industries such as catalytic converters, automotive, electronic, chemical, jewelry, dental, and glass industries [15].

Table 1 Physical properties of Platinum. [16]

Physical properties	
Atomic number	78
Atomic weight	195.084
Element category	Transition metal
Electron configuration	[Xe]4f ¹⁴ 5d ⁹ 6s ¹
Melting point	2041.4 K (1768.3°C, 3214.9°F)
Boiling point	4098 K (3825°C, 6917°F)
Density	21.45 g/cm ³

In hydrogenation reaction, platinum metal catalysts are widely used in 2 forms: 1) supported form 2) nonsupported form. The supported catalyst is recommended to obtain maximum efficiency because it shows a higher activity and greater resistance to poisoning than nonsupported catalyst [11].

2.3 TiO₂ support

Titanium dioxide (TiO₂), also known as titanium(IV)oxide or titania, is the naturally occurring oxide of titanium [17]. TiO₂ is a simple inorganic compound existing in three different crystalline polymorphs shown in **Figure 1**, namely: anatase (tetragonal), rutile (tetragonal), and brookite(orthorhombic) [18]. There are three titanium atoms around each oxygen atom and six oxygen atoms around each titanium atom [19]. Anatase and rutile are the most common types. The crystalline size of rutile is always larger than the anatase phase and the most stable phase, whereas anatase and brookite phase will transform to rutile phase at a temperature above 600°C [6]. Rutile is the most stable phase at ambient pressure and temperature in macroscopic sizes while anatase is more stable in nanoscopic sizes. The most popular titania used as support in many fields is P-

25, which is commercial support contain anatase and rutile phase. TiO_2 is very interesting support for hydrogenation reactions because, after high-temperature reduction, TiO_2 shows the strong metal support interaction (SMSI). TiO_2 is widely used in several fields, such as solar cell, photocatalysts, sensors, hydrogenation, and dehydrogenation because it is nontoxicity, relatively nonreactive, long-term photostability, and high effectiveness [6]. In metal heterogeneous catalysis, anatase is frequently used as catalyst support than rutile, due to it has a high specific surface area and strong interaction with metal nanoparticles.

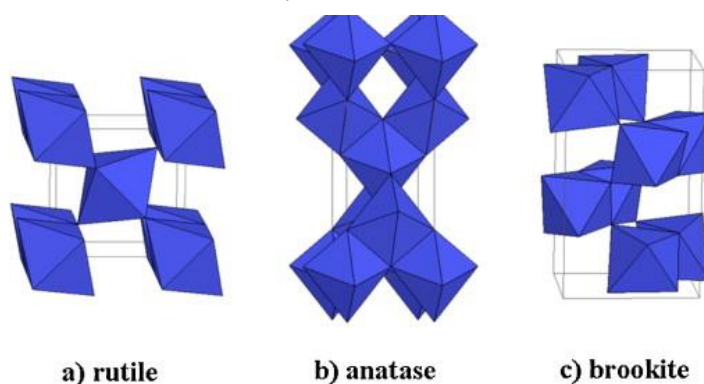


Figure 1 TiO_2 crystal structures: rutile (a), anatase (b) and brookite (c) [20]

2.4 Sol-gel

The sol-gel process is a method for producing solid materials from a small molecule. The method is used for the fabrication of metal oxides, especially the oxide of silicon and titanium [21]. A sol is a stable suspension of colloidal solid particle in the liquid phase. A gel is a porous three-dimensional inter-connected solid network and is transport due to smaller sized particles. In general, the sol-gel process involves the transition of a system from a liquid 'sol' into solid 'gel' phase. The advantages of sol-gel processing such as the production of a powder material having a high surface area, need simple equipment and low temperature of preparation and the absence of grinding and pressing step make high chemical purity which can be maintained product. But this process has some disadvantages also such as long processing time, the high cost of precursors and the possibility of the formation of hard agglomerates [22].

2.5 Strong metal-support interaction (SMSI)

The strong metal-support interaction (SMSI) is the interaction between metals and oxide supports, that important in heterogeneous catalysis and electrocatalysis. SMSI shows important differences in catalytic activity and selectivity. When the VIII groups metals supported on reducible supports are treated by a high-temperature reduction process [23]. The support is reducible which SMSI commonly appears at the metal-support interface such as TiO_2 , CeO_2 , Nb_2O_5 [24], and V_2O_3 [25].

Colmenares, C.J. et al. (2011) [25] Studied the influence of the SMSI of Pt/TiO_2 and Pd/TiO_2 in the photocatalytic biohydrogen production from glucose solution. XPS characterization of systems showed the result of thermal treatment at 850°C , the electron transfer from titania to metal particles through the strong metal-support interaction (SMSI) effect.

2.6 Hydrogenation of furfural to furfuryl alcohol

Furfuryl alcohol (FA) is the main product from the selective hydrogenation of furfural. FA as an ingredient in the manufacture of various chemical products, such as vitamin C, lysine, plasticizer, dispersing agent, lubricant, adhesives, resin and wetting agents (**Figure 3**) [26]. The selective hydrogenation of furfural consists of two function group is $\text{C}=\text{C}$ double bond and $\text{C}=\text{O}$ double bond. To produce FA, furfural is hydrogenated at $\text{C}=\text{O}$ bond to get FA as shown in **Figure 2**. In this reaction, when using methanol as a solvent, 2-furaldehyde dimethyl acetal that is the side reaction product which occurred from the methanol reaction forming solvent product (SP) was observed [4].

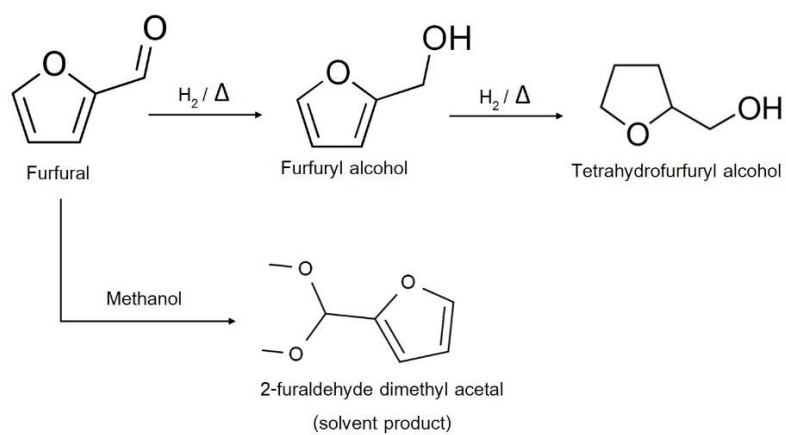


Figure 2 Simplified reaction scheme of the hydrogenation of furfural.

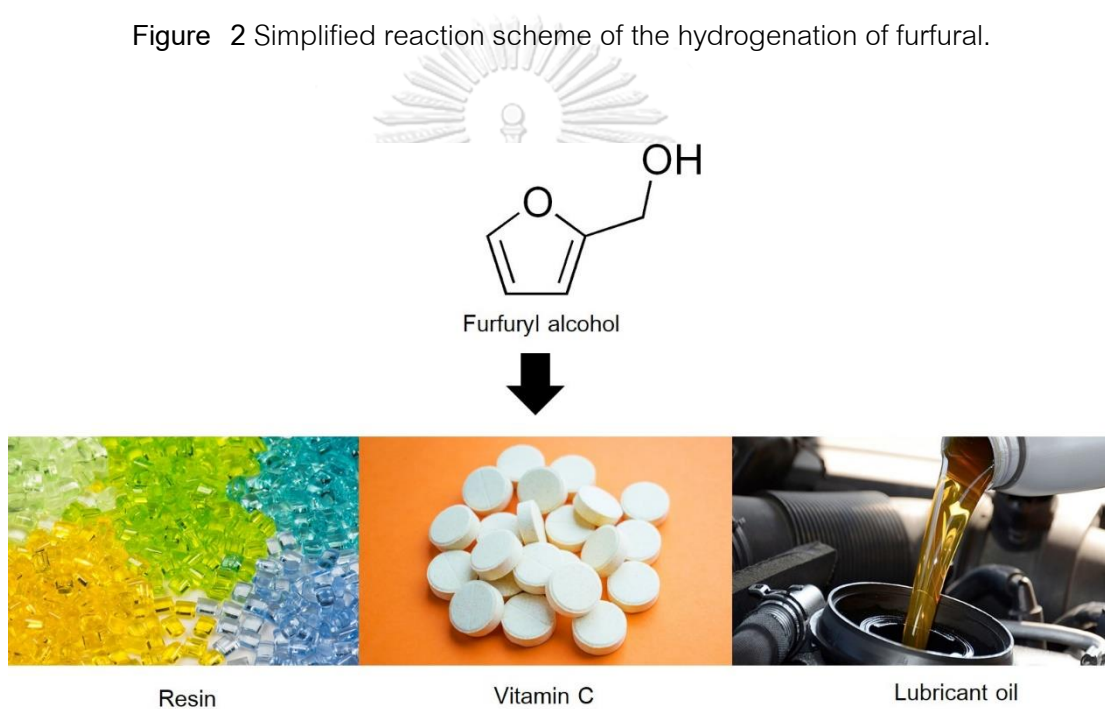


Figure 3 Application of furfuryl alcohol

Table 2 Summary of the research of the furfural hydrogenation on various catalysts under different reaction condition.

Ref.	Summary	Catalyst and preparation method	Reaction conditions	Significant findings
Taylor, M.J. et al. (2016) [4]	Studied the selective liquid phase hydrogenation of furfural to furfuryl alcohol over Pt nanoparticle supported on SiO ₂ , ZnO, γ-Al ₂ O ₃ , CeO ₂ and various solvents under extremely mild conditions.	Pt/ SiO ₂ , Pt/ZnO, Pt/γ-Al ₂ O ₃ , Pt/CeO ₂ were prepared by adapting the method of Jones et al.	T = 50°C P _{H2} = 1 atm Reaction time = 7 h	Pt/γ-Al ₂ O ₃ showed the highest furfural conversion 80% and furfuryl alcohol selectivity 99% in methanol solvent.
Zhang, C. et al. (2017) [27]	Studied the effect of bimetallic overlayer catalysts (Ni-Pt/SiO ₂ and Cu-Pt/SiO ₂) and monometallic catalysts	-Ni-Pt/SiO ₂ and Cu-Pt/SiO ₂ were synthesized using incipient wetness impregnation -Ni-Pt/SiO ₂ and Cu-Pt/SiO ₂ were prepared by the directed deposition technique.	T = 250°C P _{H2} = 6.8 atm Reaction time = 1.5 h	-Ni-Pt/SiO ₂ and Cu-Pt/SiO ₂ overlayer catalysts showed higher reactivity in furfural conversion compared to parent metals.

	(Ni/SiO ₂ , Cu/SiO ₂ , Pt/SiO ₂) for furfural hydrogenation .			- Cu-Pt/SiO ₂ overlayer catalysts showed high furfuryl alcohol selectivity.
Kijenski, J. et al. (2002) [28]	Studied the effect of platinum catalysts on supports (SiO ₂ , γ -Al ₂ O ₃ , MgO, TiO ₂) covered with a transition metal oxide monolayer (TiO ₂ , V ₂ O ₅ , ZrO ₂) in hydrogenation of furfural to furfuryl alcohol.	Pt/SiO ₂ , Pt/ γ -Al ₂ O ₃ , Pt/MgO, Pt/TiO ₂ were prepared by dry impregnation method.	T = 150°C P _{H₂} = 1 atm Reaction time = 0.5 h	-Pt/TiO ₂ /SiO ₂ showed 93.8% of furfuryl alcohol selectivity. -The role of SMSI effects in catalyst activity and selectivity enhancement.
Driscoll, O.A. et al. (2016) [29]	Studied the liquid-phase hydrogenation of furfural to furfuryl alcohol using Pt-	Pt-Sn/SiO ₂ catalyst was prepared by co-impregnation method	T = 100°C P _{H₂} = 20 atm Reaction time = 5 h	-Calcination of the catalyst at 450 °C gave the highest furfural conversion.

	Sn/SiO ₂ catalyst by co-impregnation method with various temperature calcination and solvent.			-0.7%Pt-0.3%Sn/SiO ₂ catalysts showed suitability for application as an industrial catalyst. -An aprotic solvent (toluene and propanone) gave the high selectivity to furfuryl alcohol.
Bhogeswararao, S. et al. (2015) [1]	Studied hydrogenation of furfural over γ -Al ₂ O ₃ supported Pt and Pd catalysts.	Pt/ γ -Al ₂ O ₃ and Pd/ γ -Al ₂ O ₃ were prepared by wet impregnation method.	T = 25°C, 180°C, 210°C, 240°C P _{H₂} = 20 atm Reaction time = 5 h	-At T 25°C, Pt catalysts were selective of C=O group but Pd catalysts hydrogenated both ring and C=O groups. - At higher temperature (T ≥ 180°C), Pd catalysts

				enabled decarbonylation of furfural giving furan 82% yield.
Liu, L. et al. (2017) [12]	Studied hydrogenation of furfural in liquid phase using ethanol as a solvent and using Nano-Pt and Nano-Pd particles to modified multiwalled carbon nanotubes catalysts	MWNT Supported bimetallic Pt-based and Pd-based catalysts were prepared by co-impregnation method.	T = 100°C P _{H₂} = 30 atm Reaction time = 5 h	Pt-Fe/MWNT and Pd-Ni/MWNT catalysts were used to enhance the catalytic activity for furfural hydrogenation.
Vargas-Hernandez, D. et al. (2013) [30]	Studied effect of copper (Cu) supported on SBA-15 silica catalysts in vapor phase, with various Cu loadings (8, 15, and 20	SBA-xCu catalysts were prepared by impregnation method by various Cu loadings (8, 15, and 20 wt%).	For SBA-15Cu T = 170-270°C Reaction time = 1 h	The SBA-Cu with the 15 wt% Cu catalyst shows better catalytic performance reaching a 91.5% furfural conversion

	wt%).			and 93.1% selectivity to furfuryl alcohol.
Salnikova, K. et al. (2018) [31]	Studied the palladium catalysts with different supports (aluminum oxide, hyper crosslinked polystyrene, and magnetite/ hyper crosslinked polystyrene) in the selective hydrogenation of furfural to furfuryl alcohol.	3% Pd/Al ₂ O ₃ , 3% Pd/HPS, and 3 % Pd/Fe ₃ O ₄ /HPS were prepared by impregnation method	T = 120°C P _{H₂} = 59 atm Reaction time = 4 h	The most effective catalyst was magnetically recoverable 3% Pd/Fe ₃ O ₄ /HPS give >95% conversion of furfural and 94% selectivity for furfuryl alcohol.
Chen, X. [10] (2016)	Studied the selective hydrogenation of furfural to furfuryl alcohol over Pt	Pt/ g-C ₃ N ₄ prepared by ultrasound-assisted reduction method.	T = 100°C P _{H₂} = 9.8 atm Reaction time = 5 h	-The g-C ₃ N ₄ nanosheets with the high surface area were demonstrated

	<p>catalysts supported on graphitic carbon nitride nanosheets (g-C₃N₄) in water.</p>			<p>to be excellent support for Pt nanoparticle loading.</p> <p>- 5% Pt/ g-C₃N₄ give >99% conversion of Furfural and high selectivity of furfuryl alcohol.</p>
<p>Chen, B. (2015) [32]</p>	<p>Studied the effect of supported bimetallic catalysts in liquid-phase hydrogenation of furfural.</p>	<p>Pt-Re/TiO₂-ZrO₂, Pt-In/TiO₂-ZrO₂, and Pt-Sn/TiO₂-ZrO₂ were prepared by co-impregnation method.</p>	<p>T = 130°C P_{H₂} = 49.3 atm Reaction time = 8 h</p>	<p>-Pt-Re bimetallic catalyst is an excellent partial hydrogenation catalyst for furfural conversion.</p> <p>-Furfural is converted and the selectivity of partial hydrogenation product (furfuryl</p>

				alcohol) reaches 95.7%.
--	--	--	--	-------------------------------

The research of furfural hydrogenation on various catalysts under different reaction condition as shown in **Table 2**. Cu metal was popular in the hydrogenation of furfural. Vargas-Hernandez, D. et al. (2013) [30] studied the effect of copper (Cu) supported on SBA-15 silica catalysts in the vapor phase, with various Cu loadings (8, 15, and 20 wt%). The catalysts were prepared by impregnation method. From the result, the SBA-Cu with the 15 wt% Cu catalyst shows a better catalytic performance reaching a 91.5% furfural conversion and 93.1% selectivity to furfuryl alcohol after 5 h at 170°C. The catalytic performance has demonstrated from the higher conversion at low reaction temperature and by using high catalyst weight and low furfural feed because of the evaluation of the effect of different reaction parameters such as reaction temperature (170-270°C), catalyst loadings and furfural concentration. According to Salnikova, K. et al. (2018) [31] 3% Pd/Al₂O₃, 3% Pd/HPS, and 3 % Pd/Fe₃O₄/HPS were investigated in furfural hydrogenation. It was found that the nature of support has a significant effect on the conversion of furfural and the selectivity for furfuryl alcohol. The most effective catalyst was the magnetically recoverable 3% Pd/Fe₃O₄/HPS give >95% conversion of furfural and 94% selectivity for furfuryl alcohol.

Pt metal was also popular in furfural hydrogenation to furfuryl alcohol because Pt selective to hydrogenate the C=O bond. Bhogeswararao, S. et al. (2015) [1] synthesized the γ -Al₂O₃ supported Pt and Pd catalysts for furfural hydrogenation. Furfural was hydrogenated at 25°C using γ -Al₂O₃ supported Pt and Pd catalysts. It was found that Pt catalysts were selective for hydrogenation of C=O group (producing furfuryl alcohol) but Pd catalysts hydrogenated both ring and C=O group (producing furfuryl alcohol and tetrahydrofurfuryl alcohol). At higher temperature, Pd catalysts enabled decarbonylation of furfural giving furan 82% yield. Under the reaction conditions used (furfural 1 g, isopropanol as a solvent 20 g, H₂ pressure 20 bar, catalyst 0.05g, temperature 240°C and

reaction time 5 h), the supported Pt catalysts facilitated hydrogenolysis of C=O and C-O groups enabling 2-methylfuran and furan ring-opened products. Kijenski, J. et al. (2002) [28] studied the effect of platinum catalysts on supports (SiO_2 , $\gamma\text{-Al}_2\text{O}_3$, MgO , TiO_2) covered with a transition metal oxide monolayer (TiO_2 , V_2O_5 , ZrO_2) in the hydrogenation of furfural to furfuryl alcohol. Silica and titania were found to be the most suitable supports for platinum catalysts containing the monolayers of transition metal oxide. From the result, the catalysts supported MgO gave good selectivity, but the activity of this system was low. The $\gamma\text{-Al}_2\text{O}_3$ was found to be the least appropriate carrier for supported platinum catalysts because the main reaction gave the resins as a product. The electronegativity of transition metals (Ti 1.4; Zr 1.5; V 1.7) and platinum are 2.2. If electronegativity of platinum and transition metal were different, this leads to the highest selectivity of Pt/ TiO_2 /metal oxide carrier systems. The selectivity of platinum catalysts deposited on the supports covered with transition metal oxide monolayer changed in the order: Pt/ TiO_2 monolayer/carrier > Pt/ ZrO_2 monolayer/carrier >> Pt/ V_2O_5 monolayer/carrier. In Chen, X. (2016) [3], the graphitic carbon nitride nanosheets ($\text{g-C}_3\text{N}_4$) supported Pt catalysts were investigated in furfural hydrogenation using water as a solvent. From the results, when 5%Pt/ $\text{g-C}_3\text{N}_4$ was used as the catalyst, the reaction might mainly proceed via hydrogenation of C=O bonds to form furfuryl alcohol. The $\text{g-C}_3\text{N}_4$ nanosheets with the high surface area were demonstrated to be excellent support for Pt nanoparticle loading, significant improvement of activity with high conversion of furfural and high selectivity of furfuryl alcohol >99%.

The furfural hydrogenation is strongly sensitive to the solvent selection. Taylor, M.J. et al. (2016) [4] studied the selective liquid phase hydrogenation of furfural to furfuryl alcohol over Pt nanoparticle supported on SiO_2 , ZnO , $\gamma\text{-Al}_2\text{O}_3$, CeO_2 and various solvents under extremely mild conditions. When using ethanol and methanol as the solvent, side products of the reaction between furfural and alcohol solvent are 2-furaldehyde diethyl acetal and 2-furaldehyde dimethyl acetal. This reaction is strongly sensitive to the solvent used, with alcohols (ethanol, methanol, n-butanol) more active than non-polar solvents (toluene, hexane). Non-polar solvents conferred poor furfural

conversion, however methanol as the most suitable solvent for furfural hydrogenation. Pt particle size with approximately 4 nm (over MgO, CeO₂, and γ -Al₂O₃) is highly active and selective for the hydrogenation in methanol, depending on the support of catalysts. Smaller Pt nanoparticles present in the MgO and SiO₂ catalysts promote some decarbonylation to furan. Driscoll, O.A. et al. (2016) [29] found that an aprotic solvent (such as toluene or propanone) gave lower furfural conversion, but selectivity to furfuryl alcohol close to 100% compared protic solvent. A protic solvent (such as 1-propanol and 2-propanol) yielded higher conversion but selectivity to the desired product furfuryl alcohol was compromised with alcohol solvent. Solvent 2-propanol gave 2-furaldehyde diethyl acetal and difurfural ether by-product formation while 1-propanol gave 2-methyl furan, 2-isopropoxymethyl furan, and 2-furaldehyde dipropyl acetal by-product formation. The synthesized 0.7%Pt-0.3%Sn/SiO₂ catalyst showed the high selectivity to furfuryl alcohol and using aprotic solvent.

The bimetallic catalyst has also affected the furfural hydrogenation, bimetallic catalysts usually improve the catalytic activity compared to the monometallic catalyst. Zhang, C. et al. (2017) [27] studied the effect of bimetallic overlayer catalysts (Ni-Pt/SiO₂ and Cu-Pt/SiO₂) and monometallic catalysts (Ni/SiO₂, Cu/SiO₂, Pt/SiO₂) for furfural hydrogenation. Cu-Pt and Ni-Pt showed higher reactivity compared to their parent metals. Both catalysts showed higher reactivity because reduced binding strength of H₂ on Pt surface, resulting in fewer Pt sites being blocked by strong hydrogen adsorption and increased Pt reactivity. Also, Cu-Pt showed selectivity to furfuryl alcohol like pure Cu and higher than pure Pt. Liu, L. et al. (2017) [5] modified multiwalled carbon nanotubes catalysts via co-impregnation method. Pt and Pd catalysts used different transition metals (Cr, Mn, Fe, Co, Ni) as promoters and various supports (MWNT, AC, H-AC, MgO, γ -Al₂O₃, TiO₂, ZrO₂). MWNT support gave the most excellent catalytic activity and least byproduct could be formed compared to other supports. It was found that Pt-Fe/MWNT (Pt 0.5 wt%) catalyst is selective for hydrogenation of C=O to form furfuryl alcohol and showed highest selectivity to furfuryl alcohol, while Pd-Ni/MWNT (Pd 0.5 wt%) is beneficial for both C=C and C=O group forming tetrahydrofurfuryl alcohol and showed

highest and selectivity to tetrahydrofurfuryl alcohol. From the result, it was found the high conversion and selectivity driven by promoters could be considered from aspect is the catalytic active site interacting with promoters and the electron contribution from promoters to Pt and Pd because of the alloy, which would be interpreted by the following experiment. Chen, B. (2015) [32] studied the effect of Pt-Re/TiO₂-ZrO₂, Pt-In/TiO₂-ZrO₂, and Pt-Sn/TiO₂-ZrO₂ in liquid-phase hydrogenation of furfural. From the result, when oxide species are located on Pt surface, the hydrogen species on Pt are transferred to adsorbed C=O bond to achieve selective hydrogenation. The Pt-Re bimetallic catalyst is an excellent partial hydrogenation catalyst for furfural conversion. Furfural is converted and the selectivity of partial hydrogenation product (furfuryl alcohol) reaches 95.7%.

2.7 Effect of TiO₂ support on hydrogenation reaction

Table 3 Summary of the research on the effect of TiO₂ structure support for the hydrogenation reaction

Researcher	Purpose of the study	Results
Li, Y et al. (2004) [33]	Studied the effect of titania polymorph on the strong metal-support interaction of Pd/TiO ₂ catalyst in long-chain alkadienes hydrogenation.	Rutile more thermodynamically and structurally stable than anatase because Ti ³⁺ ions which produced by reduction of Ti ⁴⁺ in the lattice of anatase is easier to diffuse to surface of Pd particle than rutile.
Ramprakash, P. et al. (2016) [34]	Studied the selective hydrogenation of CO to methane over TiO ₂ -supported Ruthenium nanoparticles.	- Low Ru content is sufficient to achieve the best results. - Ru particles have better dispersion because good surface offered of TiO ₂ .
Rizhi, C. et al. (2006)	Studied the effect of titania structure on Ni/TiO ₂ catalysts	The catalytic activity of anatase titania supported nickel catalyst

[35]	hydrogenation of <i>p</i> -Nitrophenol to <i>p</i> -aminophenol.	Ni/TiO ₂ (A) is higher than that of rutile titania supported nickel catalyst Ni/TiO ₂ (R).
Panpronont, J. (2006) [36]	Studied the effect of TiO ₂ supports consisting of various crystalline phase composition on the physicochemical and catalytic properties of Pd/TiO ₂ in selective acetylene hydrogenation.	Pd/TiO ₂ -R44 is the best composition of the TiO ₂ used to obtain high selectivity of ethylene in selective acetylene hydrogenation because the increasing percentages of rutile phases resulted in a decrease in Brunauer-Emmett-Teller surface areas

The effect of TiO₂ structure support for the hydrogenation reaction is shown in **Table 3**. For the hydrogenation reaction, Titanium dioxide or also known as titania is the most popular support. Titania has a different crystalline phase. They are, nontoxic and have low price. Rizhi, C. et al. (2006) [35] studied the effect of titania structure on Ni/TiO₂ catalysts hydrogenation of *p*-Nitrophenol to *p*-aminophenol. Ni/TiO₂ catalysts were prepared by impregnation method. The dispersion, particle size and reduction behavior of titania supported Ni were influenced by the structure of titania. The catalytic activity of anatase titania supported nickel catalyst Ni/TiO₂(A) is higher than that of rutile titania supported nickel catalyst Ni/TiO₂(R) because the reduction of nickel oxide to metallic nickel for Ni/TiO₂(A) is easier than that for Ni/TiO₂(R). For the different crystalline phase of TiO₂ as investigated by Panpronont, J. (2006) [36] on, the effect of TiO₂ supports consisting of various crystalline phase composition on the physicochemical and catalytic properties of Pd/TiO₂ in selective acetylene hydrogenation. Pd/TiO₂ was prepared by the incipient wetness impregnation method and various TiO₂ rutile with 0-44%. It found that, Pd/TiO₂-R44 is the best composition of the TiO₂ used to obtain high selectivity of ethylene in selective acetylene hydrogenation because the increasing percentages of rutile phases resulted in decrease in Brunauer-Emmett-Teller surface

areas, fewer Ti^{3+} sites and lower Pd dispersion which the presence of Ti^{3+} in the Pd/TiO₂ catalysts appeared to promote ethylene selectivity in selective acetylene hydrogenation. In the hydrogenation reaction, the SMSI effect of TiO₂ was important. Li, Y et al. (2004) [33] studied the effect of titania polymorph on the strong metal-support interaction of Pd/TiO₂ catalyst in long-chain alkadienes hydrogenation. The pre-reduced by H₂ at lower temperature results in SMSI for anatase, but not for rutile support. Rutile more thermodynamically and structurally stable than anatase because Ti^{3+} ions which produced by reduction of Ti^{4+} in the lattice of anatase is easier to diffuse to surface of Pd particle than rutile. Pd/TiO₂ (A) reduced at lower temperature has a higher selectivity for alkenes than Pd/TiO₂ (R). The TiO₂ support give the good surface for metal dispersion. Ramprakash, P. et al. (2016) [34] studied the selective hydrogenation of CO to methane over TiO₂-supported ruthenium nanoparticles. It was found that low Ru content is sufficient to achieve the best results. Ru particles have better dispersion because good surface offered of TiO₂. From the result, TiO₂ is a good acidic support.

2.8 The effect of calcination temperature on the sol-gel synthesized TiO₂ support

Table 4 Summary of the research on the effect of calcination temperature on the sol-gel synthesized TiO₂.

Researcher	Purpose of the study	Results
Chen, J. et al. (2009) [37]	Studied the effect of calcination and reduction temperature for Ni/TiO ₂ catalysts were prepare by sol-gel method on hydrogenation of chloronitrobenzene to chloroanilline.	The calcination temperature decreases the surface area and enhances the interaction between nickel species and support, which results in a decrease of nickel active sites and catalyst performance.
Sikong, L. et al. (2007)	Studied the effect of doped SiO ₂ calcination temperature	-The phase of TiO ₂ transformation from anatase to rutile at calcination

[38]	on phase transformation of TiO ₂ photocatalyst prepared by sol-gel method.	temperature increases 600-700°C. -Anatase phase is not stable at high temperature.
Chen, T et al. (2005) [39]	Studied the effect of calcination temperature on the photocatalytic activity and adhesion of TiO ₂ films prepared by the P-25 powder-modified sol-gel method.	-In the range of 400-600°C has a sharp peak of anatase and a small peak of rutile. -When the calcination temperature reaches 700°C, most of the anatase phase has been transformed into the rutile phase.
Wang, G. et al. (2017) [40]	Studied the preparation of TiO ₂ nanoparticle and photocatalytic properties on the degradation of phenol.	-The optimal amount of DI water and absolute ethyl alcohol was 5 mL and 90 mL. -The optimal calcination temperature was 575°C. -When the temperature reached to 500°C, anatase(A) was formed. -A little rutile (R) was appeared at 575°C and became major phase at 600°C.
Su, C. et al. (2004) [20]	Studied preparation of sol-gel and photocatalysis of titanium dioxide.	-At calcination temperature 400°C, only anatase phase was observed. -When calcination temperature increased to 700°C, the rutile phase becomes greater as the major phase. -Phase transformation from anatase

		to thermodynamically more stable rutile phase when increasing the calcination temperature.
--	--	--

The effect of calcination temperature on the sol-gel synthesized TiO_2 is shown in **Table 4**. In the hydrogenation, Chen, J. et al. (2009) [37] studied the effect of calcination and reduction temperature for Ni/TiO_2 catalysts on hydrogenation of chloronitrobenzene to chloroaniline. From the results, available active sites and the catalyst performance decrease because the increase of the calcination temperature decreases the surface area and enhances the interaction between nickel species and support. Increasing the reduction temperature, the catalyst performance decreases due to the enhanced interaction between nickel species and TiO_x and the serious interaction of metallic nickel crystallites. Temperature 673 and 623 K are suitable calcination and reduction temperature. For the photocatalytic, the calcination temperatures used in sol-gel preparation affected on the photocatalysis efficiency. Su, C. et al. (2004) [20] studied preparation of sol-gel and photocatalysis of titanium dioxide. From the results, the shape of TiO_2 particles is polygonal at 400°C . At calcination temperature 400°C , only anatase phase was observed. When calcination temperature increased to 700°C , the rutile phase becomes greater as the major phase. Phase transformation from anatase to thermodynamically more stable rutile phase when increasing the calcination temperature. Anatase is more active than the rutile phase in photocatalysis. TiO_2 calcined at 500°C is the most active to catalyze but TiO_2 was calcined at 700°C showed little photocatalysis efficiency. For the TiO_2 phase, anatase phase is not stable at high temperature. Sikong, L. et al. (2007) [38], TiO_2 powders exhibit a phase transformation from anatase to rutile at calcination temperature increases $600\text{-}700^\circ\text{C}$. Anatase structures were formed at calcination temperature $300\text{-}600^\circ\text{C}$ and mixed phases of anatase and rutile were formed at temperature 700°C . The most anatase phase has been transformed into the rutile phase at temperature 700°C was investigated by Chen, T et al. (2005) [39], From characterization, In the range of $400\text{-}600^\circ\text{C}$ has a sharp peak

of anatase at 25.4° and a small peak of rutile at 27.5° . When the calcination temperature reaches 700°C , the peak of anatase decrease and the peak of rutile significantly increases. Wang, G. et al. (2017) [40] studied the preparation of TiO_2 by sol-gel method with various factors such as the amount of DI water and absolute ethyl alcohol and calcination temperature. From the result, the optimal amount of DI water and absolute ethyl alcohol was 5 mL and 90 mL. The optimal calcination temperature was 575°C from calcination at 300°C , 400°C , 500°C , 525°C , 550°C , 575°C , and 600°C for 4h. When the calcination temperature was 300°C , TiO_2 did not generate crystal. When the temperature reached to 500°C , anatase(A) was formed. A little rutile (R) was appeared at 575°C and became major phase at 600°C . (see Figure 4) The degradation at 600°C with rutile phase has low photocatalytic activity, the highest activity was observed at 575°C .

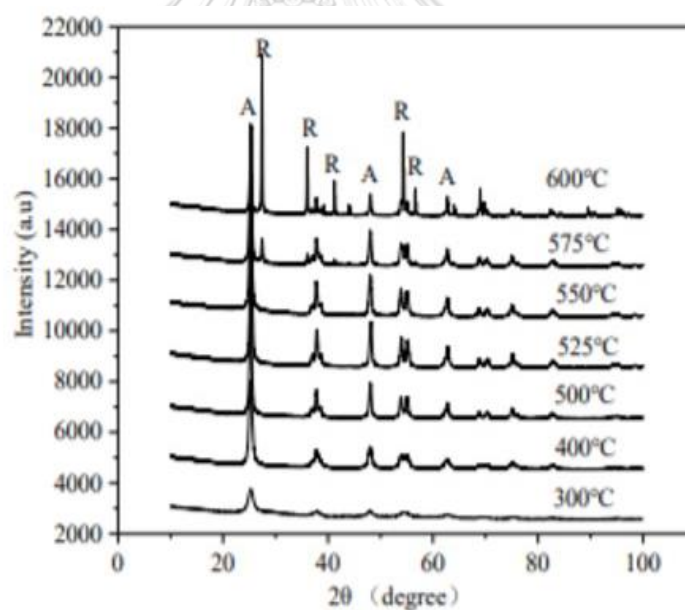


Figure 4 The XRD patterns of TiO_2 nanoparticle

CHAPTER III

MATERIALS AND METHODS

3.1 Catalyst preparation

3.1.1 Preparation of TiO₂ supported Pt catalysts.

The Pt/TiO₂ catalysts were prepared by incipient impregnation method using different polymorphs of TiO₂ as supports as shown in **Figure 5**. Platinum acetylacetonate was dissolved in xylene (MERCK; 99.8 vol%) with concentration 0.214 mol/l and dropped into each different TiO₂ polymorph (P-25, pure anatase TiO₂ with different surface areas and rutile TiO₂ with different surface areas) to get a 0.5 wt% Pt/TiO₂. Then the catalysts were dried overnight at 110°C and calcined in air at 400°C for 4 h. Finally, the catalysts were reduced at 500°C in flowing H₂ for 2 h. Chemicals used for catalyst preparation according to **Table 5** and support used according to **Table 6**.

Table 5 Chemicals used for catalyst preparation (incipient impregnation method)

Chemicals	Formula	Suppliers
Platinum (II) acetylacetonate 99.99%	Pt(C ₅ H ₇ O ₂) ₂	Aldrich
Xylene 99.8%	C ₈ H ₁₀	Merck

Table 6 Support used for catalyst preparation (incipient impregnation method)

Chemicals	Formula	Suppliers
P25	TiO ₂	DEGUSSA
Anatase (A1)	TiO ₂	Aldrich
Anatase (A2)	TiO ₂	Alfa Aesar
Rutile nanoparticle (R1)	TiO ₂	Aldrich
Rutile (R2)	TiO ₂	Aldrich

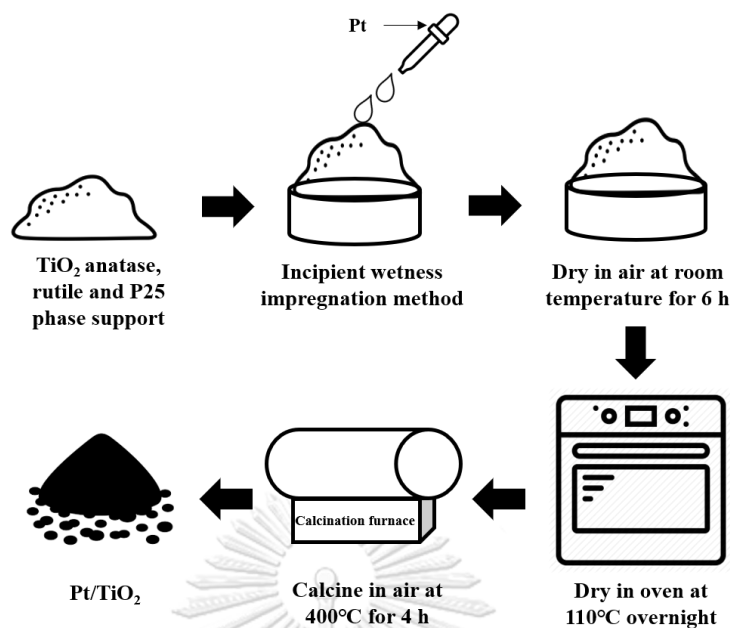


Figure 5 Diagram of Pt on TiO₂ catalysts preparation by incipient wetness impregnation method.

3.1.2 Preparation of TiO₂ sol-gel support

The TiO₂ sol-gel support was prepared by sol-gel method using titanium isopropoxide (TTIP) as a precursor, in deionized water (DI water) containing 70 vol.% nitric acid in a volume ratio of TTIP: DI water: HNO₃ was 1: 12: 0.087 according to Table 7 under constant stirring. After adding TTIP into the mixture under stirring, white precipitate was formed. The mixture stirring was conducted at room temperature for 3 days until clear sol was obtained. The clear sol was then taken and was dialyzed in cellulose membrane in DI water for 3-4 days. DI water was changed every day until the pH of the sol was 3.3-3.5. Finally, the sol was dried in an oven at 110°C overnight for remove solvent. After that, the dried sol was calcined in air at 400, 500, 600, 700°C for 2 h with a heating rate of 10°C/min to give TiO₂ powder as shown in Figure 6.

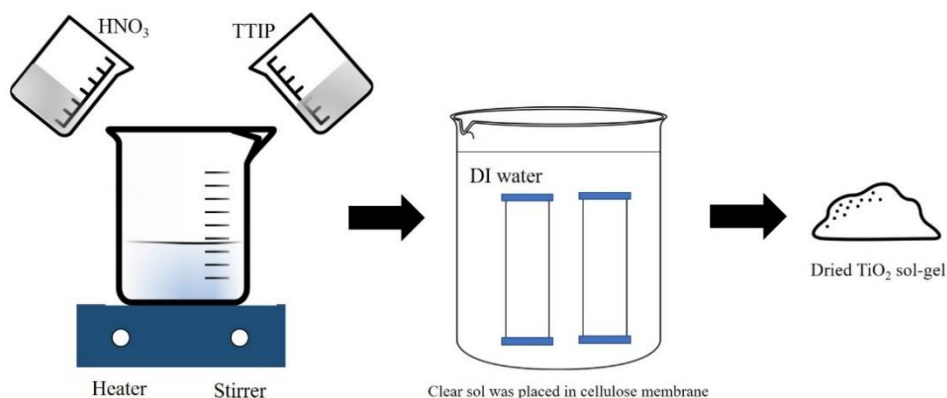


Figure 6 Diagram of TiO_2 catalyst preparation by sol-gel method

Table 7 Chemical used for TiO_2 preparation by sol-gel method

Chemicals	Formula	Suppliers
Titanium isopropoxide	$\text{Ti}[\text{OCH}(\text{CH}_3)_2]_4$	Aldrich
70% nitric acid	HNO_3	Asia Pacific Specialty Chemical limited

3.1.3 Preparation of TiO_2 sol-gel support Pt catalysts

The 0.5 wt% Pt/ TiO_2 catalysts were prepared by incipient impregnation method using sol-gel of TiO_2 as supports. Platinum acetylacetonate was dissolved in xylene (MERCK; 99.8vol%) and dropped into each TiO_2 to get a 0.5 wt% Pt/ TiO_2 . Then the catalysts were dried overnight at 100°C and various temperature calcined in air at $400, 500, 600$ and 700°C for 4 h. Finally, the catalysts were reduced at 500°C in flowing H_2 for 2 h.

3.2 Catalytic test in the selective hydrogenation of furfural

The selective hydrogenation of furfural to FA were tested in liquid phase by using the various catalysts in a 100 mL stainless steel autoclave reactor (JASCO, Tokyo, Japan) as shown in Figure 7. 0.05 g of catalyst, 50 μL of furfural and 10 mL methanol according to Table 8 were loaded into autoclave reactor supplied with a hot plate and magnetic stirrer. Then heating the water bath set at 50°C , after that purged the

autoclave reactor with H₂ for 3 times. The furfural hydrogenation reaction was carried out at 50°C, 20 bars of H₂ for 2 h and stirring mixture with a magnetic stirrer at 900 rpm. After the reaction, the reactor was cooled down to 20°C with ice-water and carefully depressurized. The reaction mixture was centrifuged and separated from the catalyst. The liquid product was analyzed by a gas chromatograph equipped with a Rtx®5 column and a FID detector according to Table 9.

Table 8 Chemicals used in the liquid-phase furfural hydrogenation

Chemicals	Formula	Suppliers
Furfural 99%	C ₅ H ₄ O ₂	Aldrich
Furfuryl alcohol 99%	C ₅ H ₆ O ₂	Aldrich
Tetrahydrofurfuryl alcohol 98%	C ₅ H ₁₀ O ₂	Aldrich
Methanol 98%	CH ₃ OH	Aldrich

Table 9 Gas-Chromatography operating conditions

Gas chromatography (Shimadzu GC-2014)	Conditions
Detector	FID
Packed column	Rtx®5
Carrier gas	Helium (99.99 vol%)
Make-up gas	Air (99.9 vol%)
Column temperature	110 °C
Injector temperature	260 °C
Detector temperature	270 °C
Time analysis	41.80 min

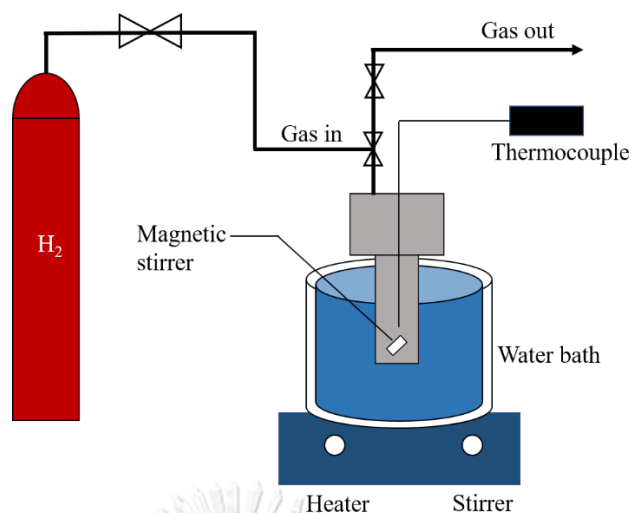


Figure 7 Schematic of the liquid-phase hydrogenation of furfural.

3.3 Catalyst Characterization

3.3.1 X-ray photoelectron spectroscopy (XPS)

The XPS spectra, the binding energy, full width at half maximum (FWHM) and the composition of Pt catalysts on the surface layer were characterized by using the Kratos AMICUS X-ray photoelectron spectroscopy. This experiment was operated with an Mg K α X-ray as a primary excitation and KRATOS VISION II software. For calibration, the binding energy of C1s peak was referenced at 285.0 eV. The binding energy (BE) of O 1s, Ti 2p, and Pt 4f are determined.

3.3.2 X-ray diffraction (XRD)

The XRD patterns were determined by a SIEMENS D5000 X-ray diffractometer with CuK α radiation in scanning range from 20° to 80° 2 θ (scan rate = 0.5 sec/step). The crystallite size was calculated using the Scherrer's equation and α -alumina as the external standard.

3.3.3 N₂-physisorption

The BET surface area, average pore size diameters, and pore size distribution of catalyst were investigated by using N₂ physisorption technique on a Micromeritics ASAP 2020 automated system.

3.3.4 Hydrogen Temperature-programmed reduction (H₂-TPR)

The H₂-TPR experiments were performed to determine reducibility and the interaction of metal and support on a Micromeritics Chemisorb 2750 with ChemiSoftTPx software. The unreduced catalyst was placed in a quartz U-tube reactor and pretreated with an N₂ flow (25 cm³/min, 1h, 250°C). Then, a gas mixture of 10% H₂/Ar was passed through the quartz reactor to the catalyst sample with a temperature ramp from room temperature to 850°C at a heating rate 10 °C/min.

3.3.5 CO pulse chemisorption

The amounts of CO chemisorbed on the catalyst, active sites, and percentages of platinum dispersion were measured from CO-pulse chemisorption technique on a Micromeritics Chemisorb 2750 with ChemiSoftTPx software. About 0.07 g of catalyst, He gas flow 25 cm³/min to removed air and then the catalyst was reduced under H₂ flow (25 cm³/min) at 500°C for 2 h with a heating rate of 10 °C/min. And cooled down to the room temperature, then He gas was inserted into the sample cell (25 cm³/min) for removed air. Next, injected 10 μL of carbon monoxide into the catalysts and replaced until the desorption peak were unchanged.

3.3.6 Transmission electron spectroscopy (TEM)

The morphology and crystallite sizes of catalysts were measured by using a JEOL-JEM 2010 transmission electron microscope using energy-dispersive X-ray detector operated at 200 kV.

CHAPTER IV

RESULTS AND DISCUSSION

In this chapter, the characteristics and catalytic properties over the Pt/TiO₂ prepared by incipient impregnation method are discussed. The results and discussion are divided into two parts. Firstly, the investigation of TiO₂ supported Pt nanoparticles prepared with different phases of TiO₂ (P-25, pure anatase TiO₂, and rutile TiO₂) for liquid phase selective furfural hydrogenation are reported. Secondly, the effect of calcination temperature of the sol-gel TiO₂ of Pt/TiO₂ catalysts for the liquid phase selective furfural hydrogenation are presented.

Part I. The investigation of the characteristics and catalytic properties of TiO₂ supported Pt nanoparticles prepared with different phases of TiO₂ in the liquid phase selective furfural hydrogenation.

4.1 The characterization of Pt/TiO₂ with different TiO₂ polymorphs.

4.1.1 X-ray diffraction (XRD)

The X-ray diffraction technique is used to analyze the structure, crystallization and phase composition of TiO₂ catalysts. The XRD patterns of catalyst samples were measured at diffraction angles (2θ) between 20° and 80° and the results are shown in **Figure 8**. All the samples showed the characteristic peaks of the crystalline phases of TiO₂ consisting of anatase phase at $2\theta = 25^\circ$ (major), 37°, 48°, 55°, 56°, 62°, 71° and 75° and rutile phase at $2\theta = 27^\circ$ (major), 36°, 42°, and 57°. The characteristic peaks of Pt cannot be detected in all the XRD patterns due to the low metal loading and/or high dispersion of these metals. The average crystallite sizes of anatase and rutile phase of TiO₂ with different supports were calculated by the Scherrer's equation from the full width at half maximum of the XRD peak at $2\theta = 25^\circ$ and 27° . The average size is summarized in **Table 11**.

The amount of anatase phase and rutile phase that was calculated from areas of a major phase of anatase ($2\theta = 25^\circ$) and rutile ($2\theta = 27^\circ$) are summarized in **Table 10**.

The Pt/TiO₂ catalysts consisting of 100, 95, 88, 6, and 7% anatase phase were called as Pt/A1, P/A2, Pt/P25, P/R1, and Pt/R2, respectively.

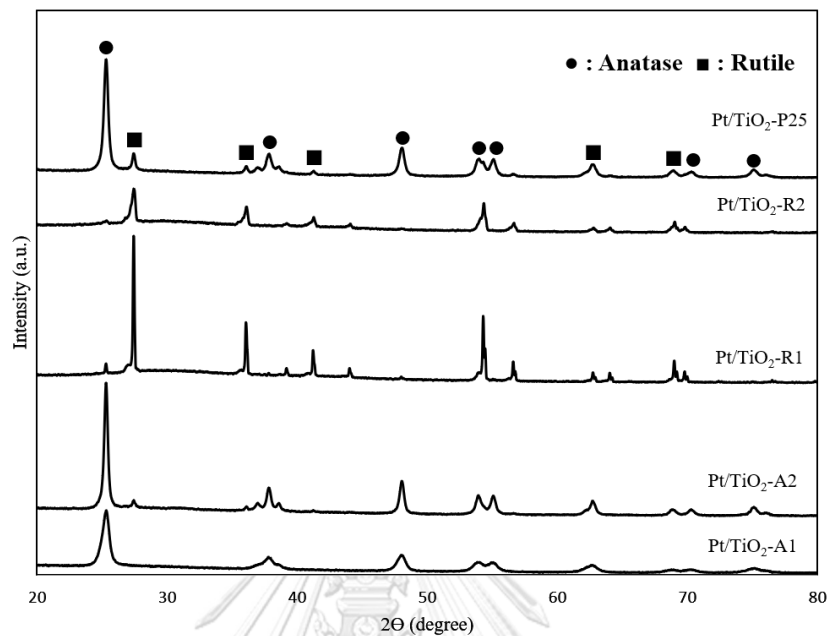


Figure 8 The XRD pattern of Pt/TiO₂ catalysts prepared with different TiO₂ polymorphs.

Table 10 Pt/TiO₂ prepared with different TiO₂ polymorphs consisting of various % anatase of TiO₂

Sample	Anatase phase ^a (%)	Rutile phase ^a (%)
Pt/ P25	86	14
Pt/ A1	100	0
Pt/ A2	94	6
Pt/R1	6	94
Pt/ R2	7	93

^aBase on the XRD results.

4.1.2 CO pulse Chemisorption

The amounts of active Pt sites and %Pt dispersion on catalyst were determined by the CO chemisorption based on the assumption that one CO molecule adsorbed on one Pt site. The catalysts were reduced at 500°C under H₂ flow before injected CO to adsorb on active sites. The %Pt dispersion and amounts of active sites of Pt/TiO₂ are shown in **Table 11**. The %Pt dispersion on Pt/TiO₂ on Pt/R1, Pt/A1, Pt/P25, Pt/A2 and Pt/R2 were 40.2%, 29.7%, 27.9%, 26.8% and 4.6%, respectively. Pt/P25, Pt/A1, and Pt/A2 were similar and higher than Pt/R2. The Pt dispersion was correlated to the BET surface area as shown in **Table 12**. Moreover, the dispersion of Pt on R2 was the lowest. According to **Table 12**, Pt/R2 has a low surface area and low pore volume when impregnation Pt sticks weakly to the R2 TiO₂ surface, which correlated to Pt actual loading. In contrast, the dispersion of Pt on R1 was the highest. Pt/R1 has a high surface area and high pore volume, which correlated to Pt actual loading.

Table 11 CO chemisorption results of Pt/TiO₂ with different TiO₂ polymorphs.

Catalyst	Pt actual loading ^a (wt%)	Amount of active sites (x10 ¹⁸) (x10 ¹⁸ molecule CO/g cat)	%Pt dispersion ^b (%)
Pt/ P25	0.46	4.3	27.9
Pt/ A1	0.48	4.6	29.7
Pt/ A2	0.48	4.1	26.8
Pt/R1	0.58	6.2	40.2
Pt/ R2	0.29	0.7	4.6

^aResult from Atomic absorption spectroscopy

^bCalculation based on Pt actual loading from atomic absorption spectroscopy

4.1.3 N₂ Physisorption

The N₂ adsorption-desorption isotherms of Pt/TiO₂ with different TiO₂ polymorphs catalysts were measured by the Brunauer Emmett Teller (BET) method and the results are shown in **Table 12**. From the results, it was found that Pt/R1 showed high BET surface area at 123.99 m²/g and large pore volume at 0.64 cm³/g as proven by the presence of the hysteresis loop of Pt/ R1 in **Figure 9**.

The N₂ adsorption-desorption isotherms of Pt/P25, Pt/A1, Pt/A2, Pt/R1, and Pt/R2 are shown in **Figure 9**. From Brunauer-Deming-Teller (BDTT), the isotherm showed type-IV physisorption isotherm of the mesoporous material with pore diameters between 2-50 nm. In addition, the shape of the hysteresis loop observed on catalysts were type H3 indicating the slit-shaped pore that was found on the pore size of solids have a very wide distribution. The Pt/R2 has low quantity N₂ adsorbed because the BET surface area, pore volume, and pore size are very low.

The BET surface area, pore volume and pore diameter of all the samples are shown in Table 12. The BET surface area of Pt/P25 and Pt/A2 were not significantly different ranging between 40-54 m²/g. The Pt/R1 had a high surface area at 124.0 m²/g and large pore volume 0.64 cm³/g that was proven by hysteresis loop of Pt/R1 in **Figure 10** because of their very small nanoparticle size.

Table 12 BET surface area, pore volume, pore diameter and average pore diameter of the catalysts

Entries	Catalyst	BET surface area (m ² /g)	Pore volume ^a (cm ³ /g)	Pore diameter ^a (nm)	Avg. crystallite size ^b of TiO ₂ (nm)	Avg. particle size of TiO ₂ from TEM (nm)
1	Pt/ P25	54.0	0.27	15.4	25	21
2	Pt/ A1	77.6	0.35	12.2	15	19
3	Pt/ A2	40.0	0.24	19.9	27	30
4	Pt/R1	124.0	0.64	16.8	15	15
5	Pt/ R2	5.3	0.007	8.1	n/a	407

* n/a: not available

^a Determined from the Barret-Joyner (BJH) desorption method.

^b Based on the XRD results.

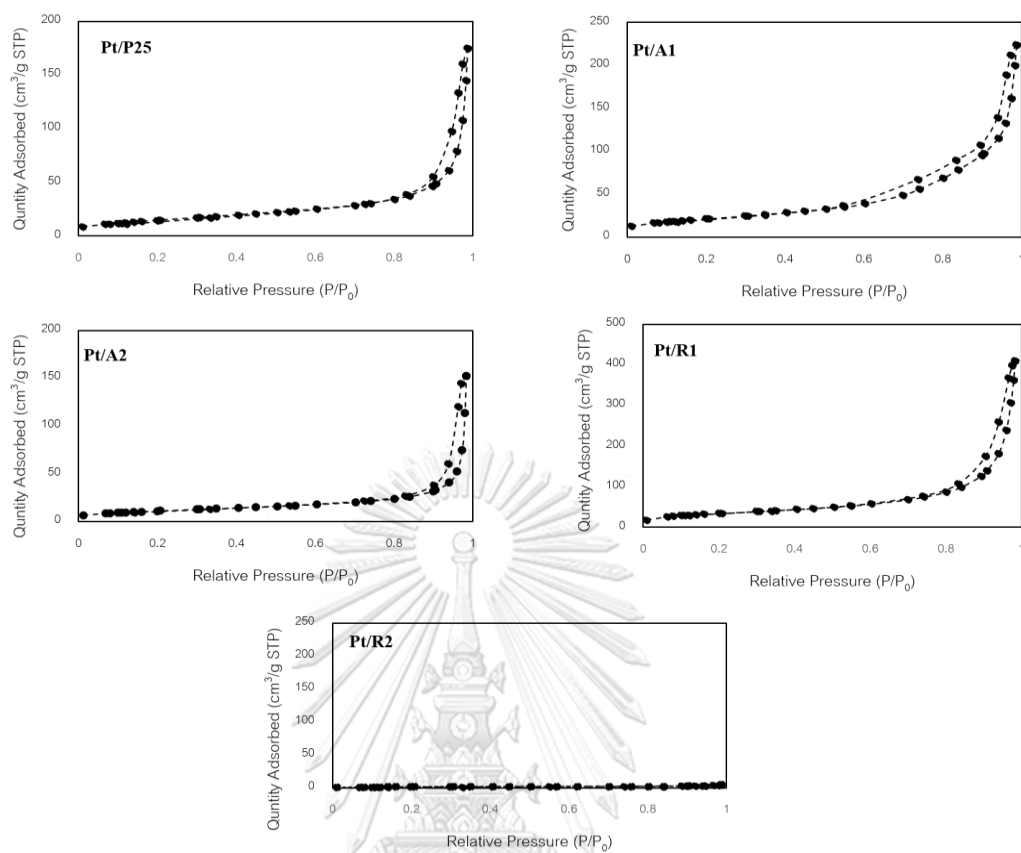


Figure 9 N_2 -Physorption isotherms of Pt/P25, Pt/A1, Pt/A2, Pt/R1, and Pt/R2

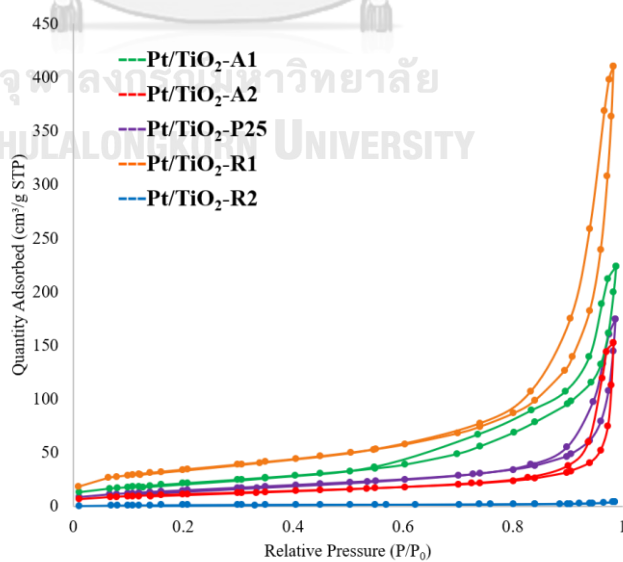


Figure 10 The combination of N_2 -Physorption isotherms of Pt/P25, Pt/A1, Pt/A2, Pt/R1, and Pt/R2

4.1.4 The H₂-temperature programmed reduction (H₂-TPR)

The H₂-TPR technique was carried out to study the reduction behaviors and, the metal and support interaction. The reduction behaviors of Pt/TiO₂ with TiO₂ phase catalysts are shown in **Figure 11**. From the results, all the Pt/TiO₂ showed three main reduction peaks at 90-107°C, 320-475°C, and 540-635°C. According to the literature, the first reduction peak around 100°C was correlated to the reduction of PtO_x crystallites to metallic Pt [41-43]. In this work, the reduction of PtO_x species at around 90-100°C were observed for all the catalysts except the Pt/A2. The reduction of PtO_x was shifted to 209°C for the Pt/A2. The reduction of PtO_x on the Pt/R2 occurred at a higher temperature compared to the other catalysts, corresponding to a lower dispersion of Pt on the support surface [44]. The second peak appeared as a larger peak around 320-472°C which could be associated with the reduction of the TiO₂ support to form Pt-TiO_x interface site and for Pt/P25, this catalyst had a higher proportion of the surface capping oxygen of TiO₂ species than Pt-TiO_x. The last peak above 500°C can be attributed to the reduction of the surface capping oxygen of TiO₂. [42] Pt/A2 had more PtO_x species than other catalysts but reduction peaks of Pt-TiO_x and TiO₂ were shifted to a higher temperature than the other catalysts. In addition, some difficult to reduce species were detected at 631°C on Pt/A2 [45].

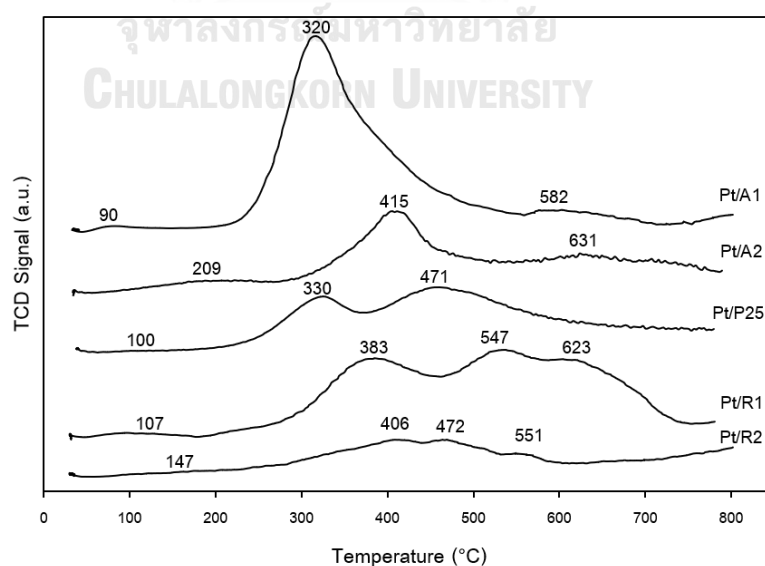
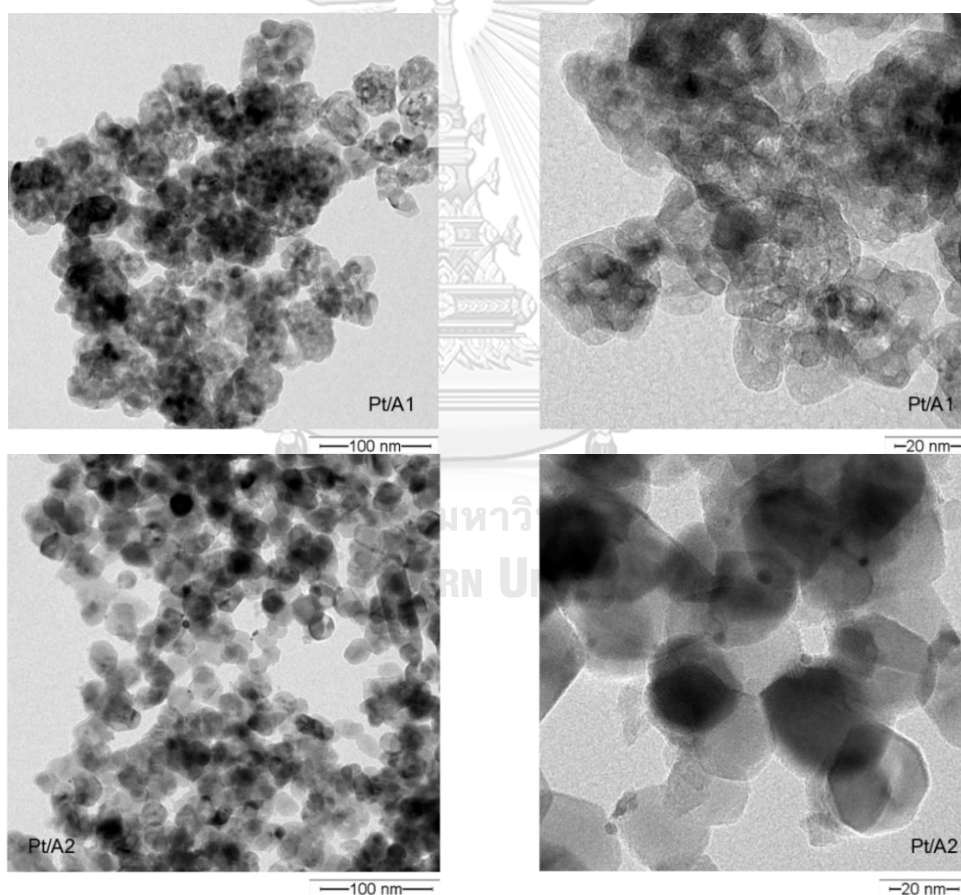


Figure 11 The H₂-TPR profiles of Pt/P25, Pt/A1, Pt/A2, Pt/R1, and Pt/R2

4.1.5 Transmission electron spectroscopy (TEM)

The morphology and particle size of catalysts can be estimated from TEM analysis. The TEM images of Pt/P25, Pt/A1, Pt/A2, Pt/R1, and Pt/R2 catalysts are shown in Figure 12, respectively. The high Pt dispersion on TiO₂ support can be confirmed by TEM. From visual observation by TEM, we can see that the crystallite size of the TiO₂ decreased in the order: R2>>A2>P25>A1>R1. The average particle size of Pt/P25, Pt/R2, Pt/A2, Pt/A1, and Pt/R1 catalysts determined from TEM image was approximately 4.8, 4.7, 2.6, 1.0 and 0.3 nm, respectively. The particle size of rutile TiO₂ was larger than the anatase phase because, the rutile consists of linear chains of opposite edge-shared octahedral structure [6, 18].



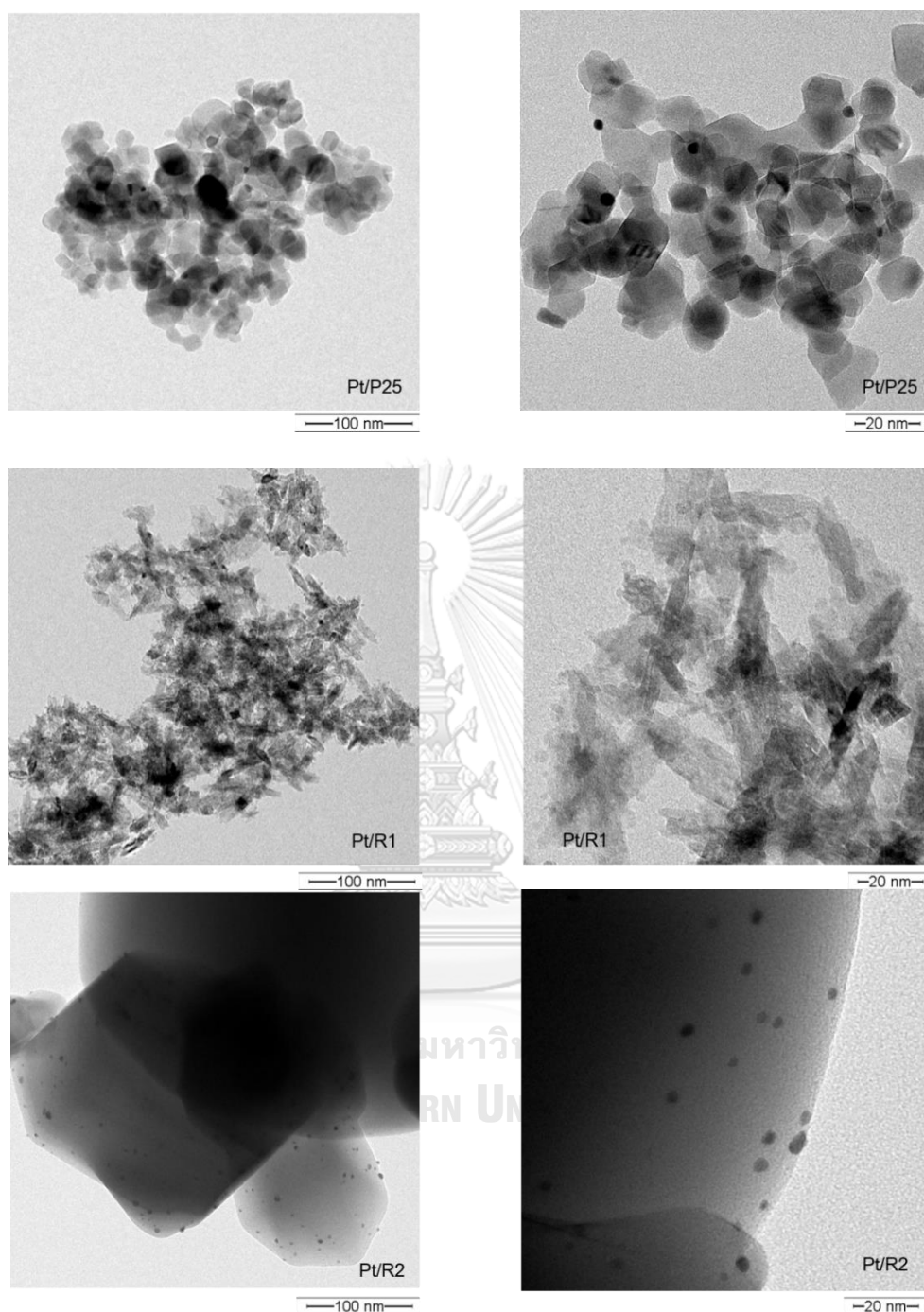


Figure 12 The TEM of Pt/P25, Pt/A1, Pt/A2, Pt/R1 and Pt/R2

4.1.6 X-ray photoelectron spectroscopy (XPS)

X-ray photoelectron spectroscopy (XPS) is a technique for detecting the element composition of catalyst. For all the catalysts sample, the XPS spectra of TiO_2 clearly showed the peaks of Ti 2p and O 1s.

The C 1S spectrum was used as an internal standard at by the binding energy of 285 eV. According to **Figure 13**, the binding energy of Ti 2p for bare TiO₂ support, the most intense was located at 458.5 eV, corresponding to Ti⁴⁺ [46]. After impregnated Pt on TiO₂ support, the XPS peak as shown in **Figure14** of Ti 2p for Pt/A1, Pt/P25, and Pt/R1 catalysts shifted to higher binding energy as compared as the bare TiO₂ support. The shift could be caused by the transfer of an electron from the TiO₂ to metallic Pt due to Pt has larger electronegativity as compared to Ti⁴⁺. It is suggested that the addition of Pt resulted in a strong interaction between the support and the active components. This evidence for Ti 2p shift to higher binding energy has also been reported on the V₂O₅/TiO₂ with different TiO₂ supports [47]. On the other hand, for Pt/A2 and Pt/R2, XPS peaks of Ti 2p shifted to lower binding energy. Similar to Chao et al.[48], the XPS Ti 2p peaks of V-TiO₂ catalysts shifted to higher binding energy, which was restored on Pt impregnation (after impregnation Pt on the V-TiO₂, the binding energy of Ti 2p was decreased and shifted to lower.) In addition, the Pt states which were observed on the Pt/TiO₂ showed the consist of Pt²⁺ and Pt⁴⁺ for Pt oxide species. It might be feasible that the oxygen contained in Pt oxides may promote the transfer of an electron to the TiO₂ support, then the binding energy of Ti 2p was decreasing.

Considering the TiO₂ support, The binding energy of O 1s for bare TiO₂ was mainly exhibited at 529.8 eV as show in **Figure 15**, which represent the lattice oxygen species in TiO₂ support [49]. After impregnated Pt on TiO₂ support, the XPS peaks as shown in **Figure 16** shifting to higher binding energy, suggesting the interaction between Pt metals and TiO₂ support. In addition, the peaks appeared at 531.6 eV, which could be attributed to surface oxygen. This O 1s peak was shifted to lower value of surface hydroxyl, suggesting the interaction between Pt and surface oxygen [50]. Moreover, on Pt/A2 and Pt/R1 O 1s peaks were detected at high binding energy at around 533.7 due to adsorbed molecular water [47].

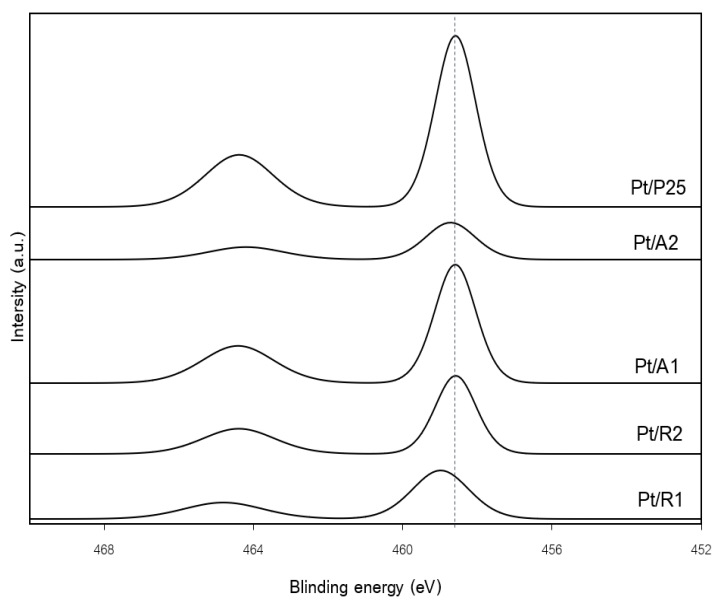


Figure 13 XPS spectra of Ti 2p of bare TiO₂ support

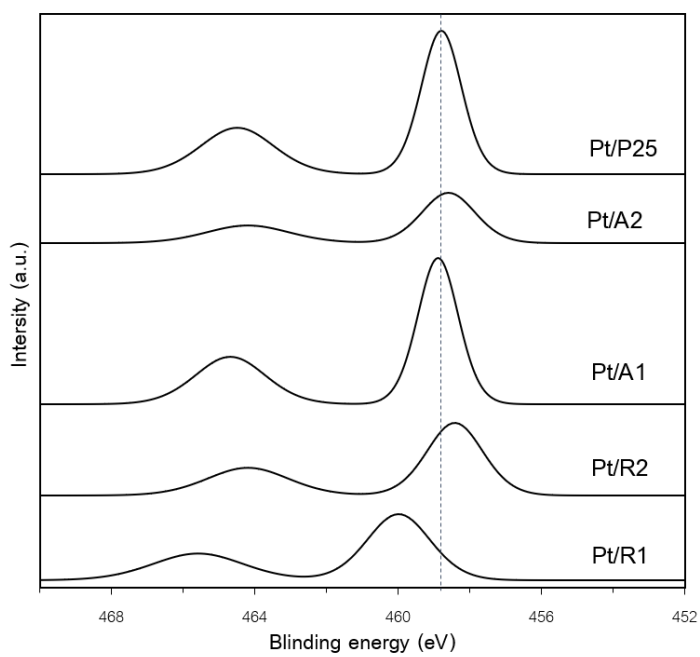


Figure 14 XPS spectra of Ti 2p of Pt/P25, Pt/A1, Pt/A2, Pt/R1 and Pt/R2

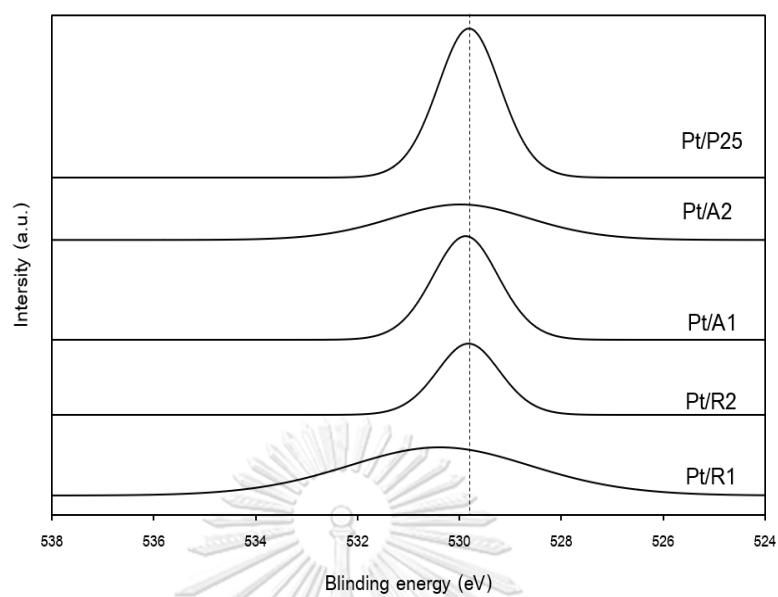


Figure 15 XPS spectra of O 1s of TiO₂ support

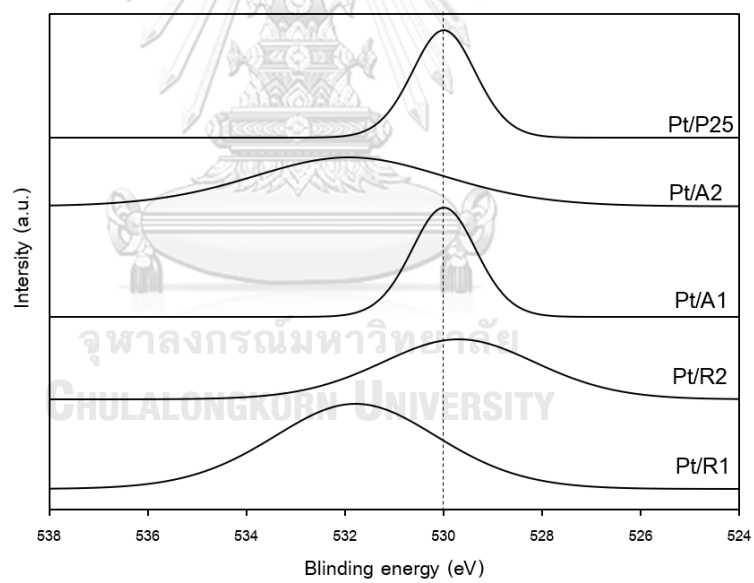


Figure 16 XPS spectra of O 1s of Pt/P25, Pt/A1, Pt/A2, Pt/R1 and Pt/R2

4.2 Evaluation of the catalyst performance in the selective furfural hydrogenation

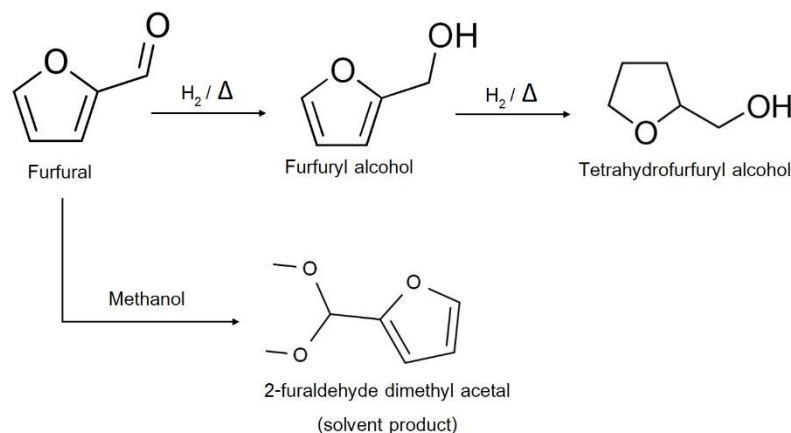


Figure 17 The pathway of furfural hydrogenation

The pathway of furfural hydrogenation reaction as shown in **Figure 17**, exhibited the two main reaction pathways. First, furfural is hydrogenated at C=O bond transformed to furfuryl alcohol (FA). After that, FA is hydrogenated at C=C bond transform to tetrahydrofurfuryl alcohol. In addition, when using methanol as a solvent, 2-furaldehyde dimethyl acetal, which a side -product of reaction or solvent product (SP) may be formed. In this work of furfural hydrogenation reaction, the desired product is furfuryl alcohol and the undesired product is 2-furaldehyde dimethyl acetal. The performances of Pt/TiO₂ prepared with different phases of TiO₂ catalysts were investigated in the selective hydrogenation of furfural at temperature 50°C at H₂ pressure 20 bars and 2 h reaction time with methanol as the solvent. The results of the selective furfural hydrogenation including the conversion of furfural and the selectivity to FA are summarized in **Table 13**.

From the results, the Pt/P25 showed the best catalytic activity among the catalysts, which may be correlated to the high Pt dispersion on P25 support as confirmed by TEM and the presence of higher amount of surface capping oxygen of the TiO₂. Considering the Pt/A1 and Pt/A2 catalysts, Pt/A1 showed higher catalytic activity than Pt/A2, which could be attributed to the anatase phase percentages. The catalytic activity decreased with the decreasing the anatase phase percentages. Moreover, Pt/A2

showed shown the worst catalytic activity, which correlated to the H₂-TPR profile that Pt/A2 did not exhibit the reduction of Pt oxides to Pt metals peak. Considering the rutile phase, the Pt/R1 and Pt/R2 catalysts showed the low catalytic activity, it could be possible that the molecular hydrogen did not interact strongly with the rutile phase of TiO₂ as atomic of hydrogen sticks to surface oxygen atom [51]. Moreover, the Pt/R1 with small sizes of Pt nanoparticles showed the lower activity than Pt/R2. The size effect of Pt has reported in the selective hydrogenation of cinnamaldehyde, the presence of low coordination sites on small sizes of Pt nanoparticles caused poor selectivity to cinnamyl alcohol [52]. In addition, the FA selectivity may not rely on the furfural conversion but rather affected by the physical properties of the catalyst supports used, the location of the metal, and the metal-support interaction.

Table 13 Reaction results of the Pt/TiO₂ catalysts.

Entries	Catalyst	Conversion (%)	Selectivity (%)		FA Yield (%)
			FA ^a	SP ^b	
1	Pt/ P25	81.0	98.3	1.7	79.7
2	Pt/ A1	36.7	94.0	6.0	34.6
3	Pt/ A2	8.8	85.2	14.8	7.5
4	Pt/ R1	14.6	88.6	11.4	13.0
5	Pt/ R2	27.8	63.4	36.6	17.6

Reaction (50 μ L furfural in 10 mL methanol) at 50^oC under 20 bars H₂ with a 50 mg catalyst for 120 min.

^aSelectivity of furfuryl alcohol

^bSelectivity of 2-Furaldehyde dimethyl acetal

Part II. Study the effect of TiO₂ support by using the sol-gel method and various temperature calcination in liquid-phase furfural hydrogenation.

4.3 The characterization of Pt/TiO₂ sol-gel with different calcination temperatures of the TiO₂.

The 0.5 wt% Pt/TiO₂ catalysts were prepared by incipient impregnation method using TiO₂ that was synthesized from the sol-gel method as supports and calcined at various temperatures in air at 400,500,600 and 700°C. The actual of Pt loading was analyzed by using the ICP technique, the results are shown in Table 14.

Table 14 The amount of Pt loading in TiO₂

Catalyst	Actual Pt loading (wt. %)
Pt/TiO ₂ -400	0.39
Pt/TiO ₂ -500	0.46
Pt/TiO ₂ -600	0.39
Pt/TiO ₂ -700	0.33

4.3.1 X-ray diffraction (XRD)

In Figure 18 shows the XRD pattern of Pt/TiO₂ catalysts with different temperature calcined TiO₂. The XRD patterns of catalyst samples were measured at diffraction angles (2θ) between 20° and 80°. The characteristic peaks of the crystalline phases of TiO₂ consisting of anatase phase at $2\theta = 25^\circ$ (major), 37°, 48°, 55°, 56°, 62°, 71° and 75°, rutile phase at $2\theta = 27^\circ$ (major), 36°, 42°, and 57° and small amount of brookite phase = at 31° [53] were detected. The diffraction peak of Pt was not observed in all XRD pattern because of low metal loading of Pt. The crystallite sizes of TiO₂ with different support grew from 8 nm to 29 nm as sintering temperature was raised from 400°C to 500°C. The average size is summarized in Table 15.

The amount of anatase phase and rutile phase that was calculated from areas of a major phase of anatase ($2\theta = 25^\circ$) and rutile ($2\theta = 27^\circ$) are summarized in Table 16. The sol-gel TiO_2 support with different temperature calcination are denoted as Pt/TiO₂-400, Pt/TiO₂-500, Pt/TiO₂-600, and Pt/TiO₂-700.

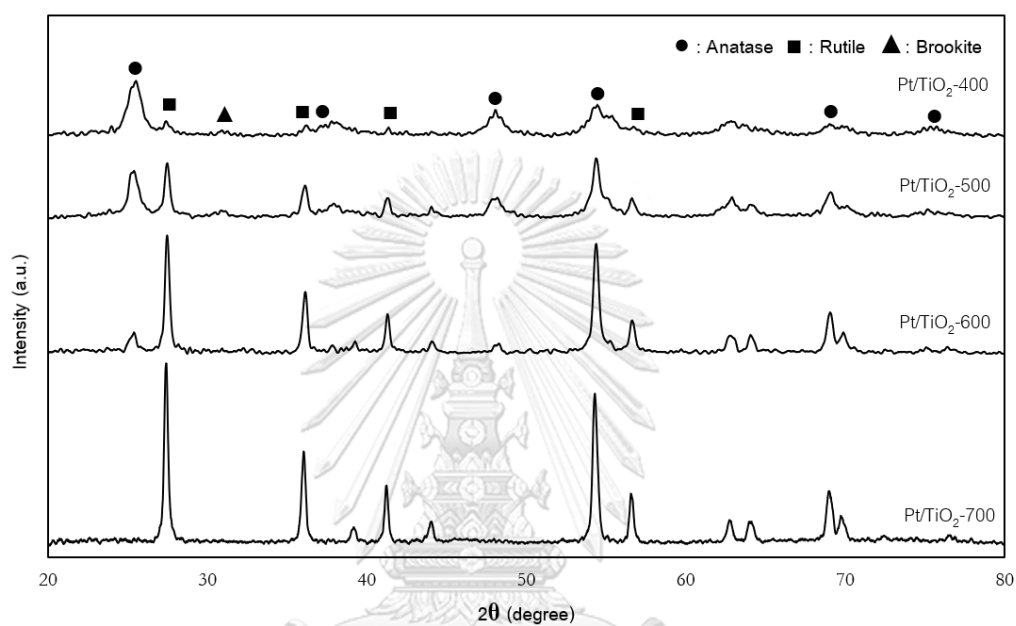


Figure 18 The XRD patterns of Pt/TiO₂ catalysts with different temperature calcined

TiO₂.

Table 15 Pt/TiO₂ prepared with different temperature calcined TiO₂ consisting of various % anatase of TiO₂

Sample	Anatase phase (%)	Rutile phase (%)	Brookite phase (%)
Pt/TiO ₂ -400	79	16	5
Pt/TiO ₂ -500	59	35	6
Pt/TiO ₂ -600	14	86	0
Pt/TiO ₂ -700	0	100	0

^aBase on the XRD results.

4.3.2 N₂-physisorption

The N₂ adsorption-desorption isotherms of Pt/TiO₂ with different temperature calcined TiO₂ are shown in **Figure 19**. According to the Brunauer-Deming-Teller (BDTT), the isotherm showed type-IV physisorption isotherm which has mesoporous material with pore diameters between 2-50 nm. The isotherms show type-IV according to the IUPAC classification, with a variant hysteresis loop in the medium to high relative pressure (P/P₀) range 0.4-1.0. Zhang, Y. et al [54] reported the presence of a large number of mesopores in the TiO₂ support. The shape of the hysteresis loop observed on catalysts was type H1 indicating to a narrow distribution of relative uniform pore. [55]. The BET surface area, pore volume and pore diameter of the Pt/TiO₂ are shown in **Table 16**. In many investigations of TiO₂ support prepared via the sol-gel method with different temperature calcinations, the surface area and pore volume decrease with calcination temperature increasing while the increase of pore diameter cause of the increase in the crystal size of TiO₂ [56]. Dodoo-Arhin, D. et al [57], reported that when calcination temperature was increased, the surface area of TiO₂ which prepared by sol-gel method rapidly decreased. Moreover, percentage of rutile phase increased whereas BET surface area was decreased [58].

Table 16 BET surface area, pore volume, pore diameter and average pore diameter of the catalysts

Entries	Catalyst	BET surface area (m ² /g)	Pore volume ^b (cm ³ /g)	Pore size ^b (nm)	Avg. crystallite size ^a of TiO ₂ (nm)	Avg. particle size of TiO ₂ from TEM (nm)
1	Pt/TiO ₂ -400	106.4	0.24	4.9	8.7	7.0
2	Pt/TiO ₂ -500	54.9	0.17	8.5	11.6	12.2
3	Pt/TiO ₂ -600	24.7	0.11	10.7	25.3	24.8
4	Pt/TiO ₂ -700	16.9	0.09	15.7	29.6	36.0

^aBased on the XRD results.

^bDetermined from the Barret-Joyner (BJH) desorption method.

^cDetermined from anatase peak at $2\theta = 25^\circ$

^cDetermined from rutile peak at $2\theta = 27^\circ$

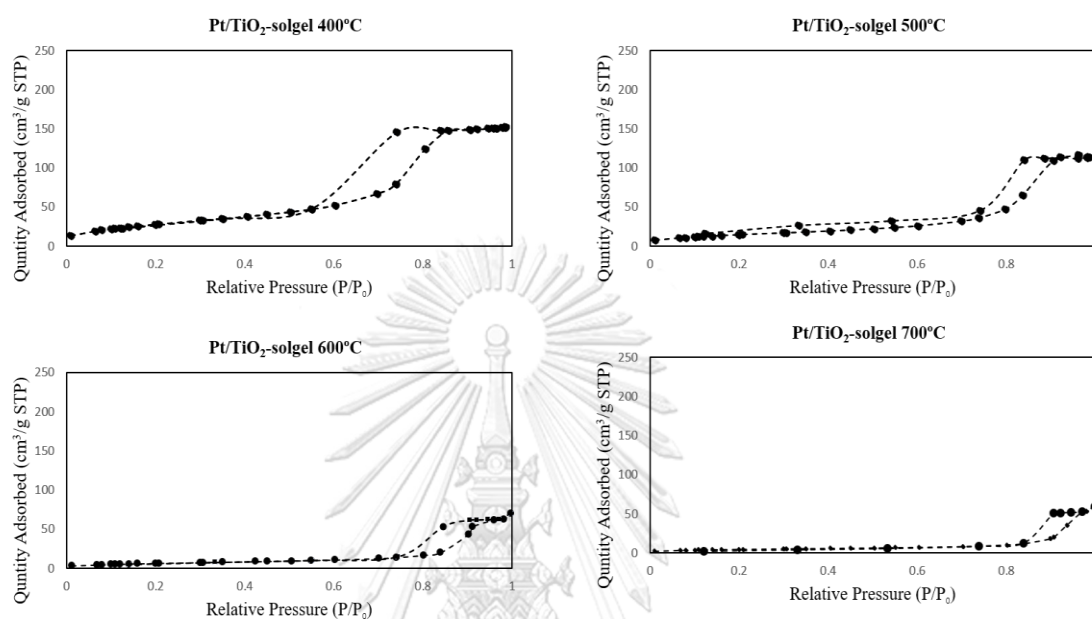


Figure 19 N₂-Physisorption isotherms of Pt/TiO₂ with different temperature calcined TiO₂.

4.3.3 The H₂-temperature programmed reduction (H₂-TPR)

The H₂-TPR measurements were carried out to study the reduction behaviors of the Pt/TiO₂ catalysts with different temperature calcined TiO₂. The results are shown in Figure 20. From the results, all the Pt/TiO₂ showed three main reduction peaks at around 100-150°C as a result of the reduction of Pt oxide to Pt metal. And at 300-465°C as a result of the reduction of Pt species interacting with the TiO₂ support to form Pt-TiO_x at interface sites. The large broad peak was observed at above 500°C, which can assign to the hydrogen consumption due to the reduction of surface capping oxygen of TiO₂.

The reduction peak of Pt/TiO₂-600 occurred at a slightly lower temperature compared to Pt/TiO₂-500 and Pt/TiO₂-700 that could be assigned to the reduction of Pt oxide to Pt metal peak occurred at a lower temperature, it makes the activity increased. However, the Pt reduction peak was not found on Pt/TiO₂-400, it might be possible that

little Pt oxide was reduced to Pt metal and as a consequence, the activity decreased as compared with the other catalysts. The second reduction peaks were shifted to higher reduction temperature when temperature calcination of sol-gel TiO_2 increased except Pt/ TiO_2 -700, suggesting stronger interaction between metal and TiO_2 support.

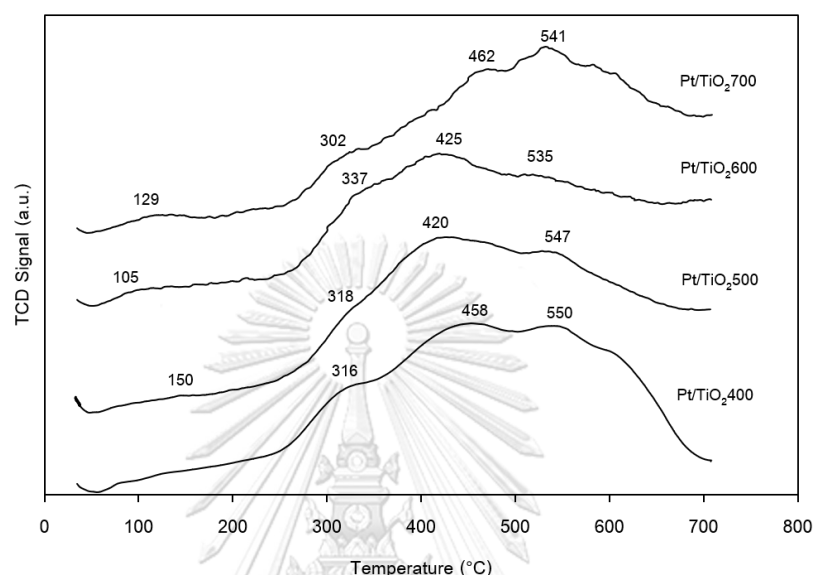


Figure 20 The H_2 -TPR profiles of Pt/ TiO_2 with different temperature calcined TiO_2 .

4.3.4 Transmission electron spectroscopy (TEM)

The TEM micrograph of the Pt/ TiO_2 -400, Pt/ TiO_2 -500, Pt/ TiO_2 -500, and Pt/ TiO_2 -600 catalysts are shown in Figure 21. The Pt well-dispersed on TiO_2 support.

The morphology and particle size of catalysts can be estimated from TEM analysis. The TEM images of Pt/ TiO_2 -400, Pt/ TiO_2 -500, Pt/ TiO_2 -500, and Pt/ TiO_2 -600 catalysts are shown in Figure 21. The high Pt dispersion on TiO_2 support can be confirmed by TEM. From visual observation by TEM, we can see that the crystallite size of the TiO_2 decreased in the order: Pt/ TiO_2 -700 > Pt/ TiO_2 -600 > Pt/ TiO_2 -500 > Pt/ TiO_2 -400. The average particle size of Pt/ TiO_2 -700, Pt/ TiO_2 -600, Pt/ TiO_2 -500, and Pt/ TiO_2 -400 catalysts determined from TEM image were approximately 2.4, 2.0, 1.8, and 1.5 nm, respectively.

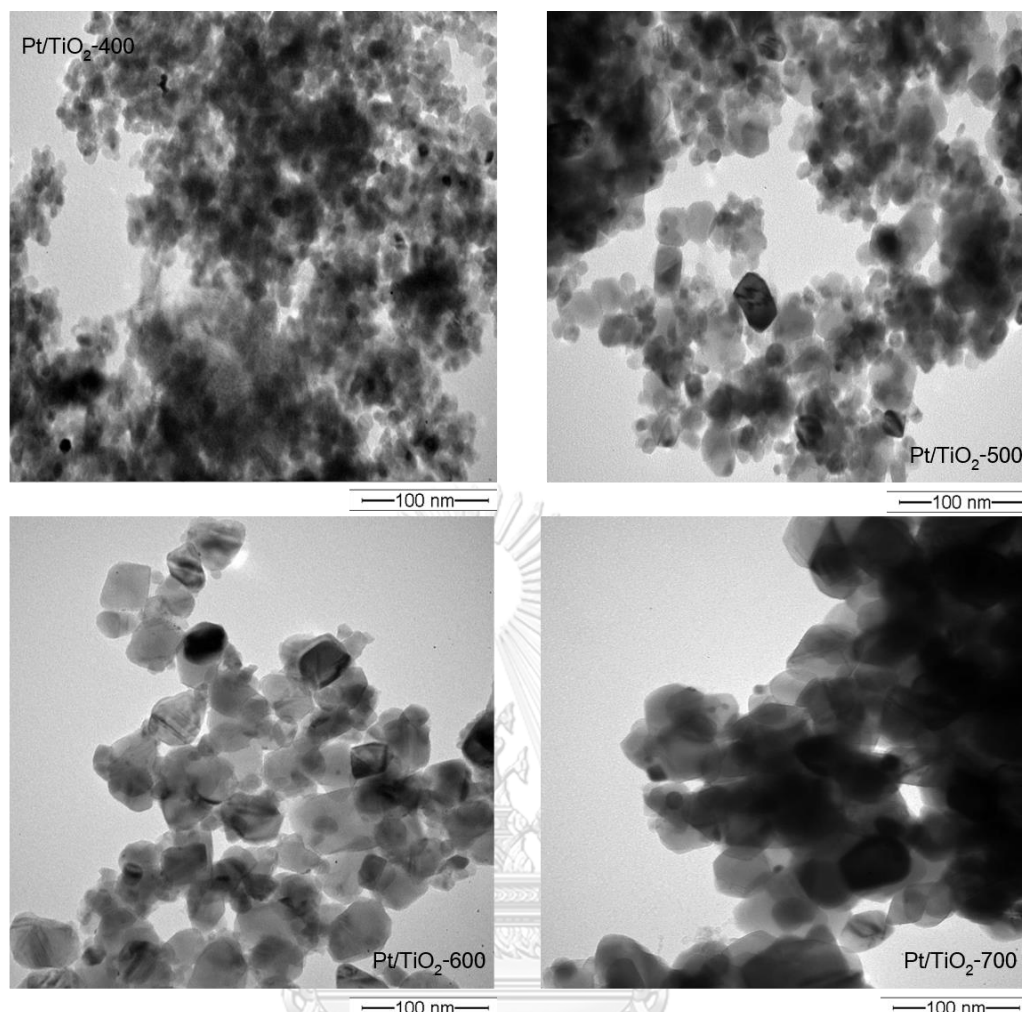


Figure 21 The TEM of Pt/TiO₂ with different temperature calcined TiO₂.

4.3.5 X-ray photoelectron spectroscopy (XPS)

The element composition of the catalyst was detected by XPS. The XPS spectra of Ti2p of Pt/TiO₂-400, Pt/TiO₂-500, Pt/TiO₂-600 and Pt/TiO₂-700 are shown in **Figure 22**. The C 1s spectrum was observed at the binding energy of 285 eV. In this work, the binding energy of Ti 2p for the Pt/TiO₂-400 and Pt/TiO₂-500 were mainly located at 458.5 eV and 464.2 eV similar to G. Li et al. [59], the Ti 2p_{3/2} and Ti 2p_{1/2} of the undoped TiO₂ appeared at 458.4 eV and 464.2 eV, respectively, indicating that Ti existed in the Ti⁴⁺ form. For Pt/TiO₂-600 and Pt/TiO₂-700, the binding energy of Ti 2p were decreased and shifted to lower. It might be possible that the electron transfer towards the TiO₂ support was promoted by oxygen in Pt oxides species, then the binding energy of Ti 2p was decreasing.

The XPS O 1s peak which shown in **Figure 23**. The O 1s region of Pt/TiO₂-400 and Pt/TiO₂-500 is composed of one peak at 529.8 eV, corresponding to Ti-O [60] or lattice oxygen in TiO₂ support [50]. This XPS peaks shifted to lower values for Pt/TiO₂-600 and Pt/TiO₂-700 similar to L Yu et al. [50], the peak shifting to lower binding energy is evidence for the interaction between Pt and surface hydroxyl.

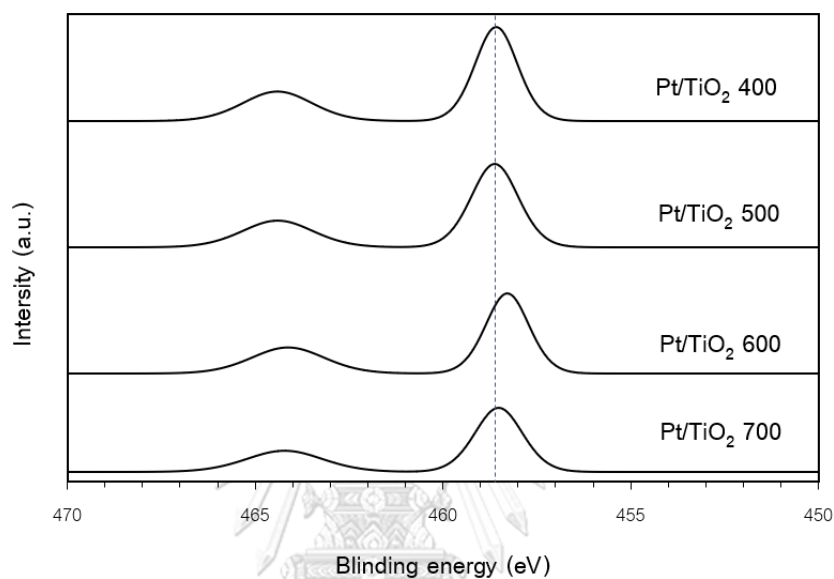


Figure 22 XPS spectra of Ti 2p of Pt/TiO₂ with different temperature calcined TiO₂.

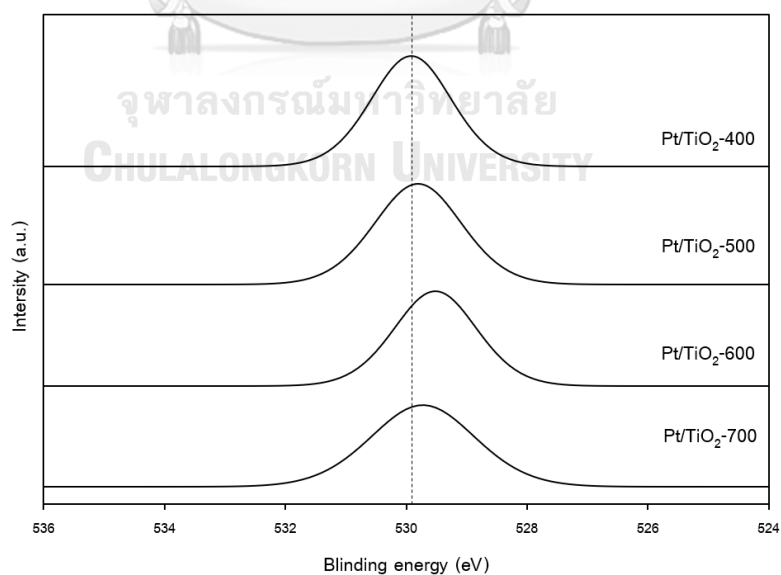


Figure 23 XPS spectra of O 1s of Pt/TiO₂ with different temperature calcined TiO₂.

4.4 The catalytic performance of Pt/TiO₂ with different temperature calcined TiO₂.

The catalytic performance of 0.5 wt% Pt/TiO₂ catalysts using TiO₂ that was synthesized from sol-gel method calcined with different temperature 400°C, 500°C, 600°C, and 700°C was investigated in the selective hydrogenation under the following reaction conditions: temperature 50°C at H₂ pressure 20 bars and 2 h reaction time with methanol as the solvent. The results are summarized in **Table 17**. In this reaction, the desired selective hydrogenation product FA was produced and the side reaction product which occurred from the methanol reaction forming solvent product (SP) was observed. From the results, the Pt/TiO₂-600 showed the best catalytic activity among the catalysts studied. According to the H₂-TPR results, the reduction peak of Pt oxide to Pt metal occurred at a lower temperature for Pt/TiO₂-600.

Table 17 Reaction results of the Pt/TiO₂ catalysts

Entries	Catalyst	Conversion (%)	Selectivity (%)		FA Yield (%)
			FA ^a	SP ^b	
1	Pt/TiO ₂ -solgel400°C	22.3	94.3	5.7	21.0
2	Pt/TiO ₂ -solgel500°C	62.3	87.4	12.6	54.5
3	Pt/TiO ₂ -solgel600°C	88.3	96.4	3.6	85.1
4	Pt/TiO ₂ -solgel700°C	41.9	89.3	10.7	37.4

Reaction (50 μ L furfural in 10 mL methanol) at 50°C under 20 bars H₂ with a 50 mg catalyst for 120 min.

^aSelectivity of furfuryl alcohol

^bSelectivity of 2-Furaldehyde dimethyl acetal

CHAPTER V

CONCLUSIONS AND RECOMMENDATION

5.1 Conclusions

The Pt/TiO₂ catalysts prepared with polymorphs of TiO₂ which different phases, crystallite sizes, BET surface area, pore volume, and pore size. For the commercially available TiO₂ supports, the Pt/P25 (mixed anatase/rutile phase) exhibited the highest catalytic activity at conversion of furfural (81%) and selectivity to furfuryl alcohol (94%). However, the Pt/TiO₂ catalysts prepared with different temperature calcination of sol TiO₂, resulted in the improved catalytic activity with the Pt/TiO₂-600 catalyst showed the best conversion of furfural (88%) with the best selectivity to furfuryl alcohol (97%). According to the H₂-TPR, XPS, and TEM results, the improved catalytic activity of both catalysts correlated well with the presence of both PtO_x species at around 100°C and Pt-TiO_x species at around 330°C, high Pt dispersion and the presence of Ti⁴⁺ in TiO₂ support. In addition, the XPS peak of Ti 2p spectra for Pt/TiO₂-600 shifted to lower binding energy, there might be electron transfer towards TiO₂ support which was promoted by oxygen in Pt oxides. In summary, Pt-based catalysts selectively produced furfuryl alcohol but different TiO₂ supports led to low or high selectivity to furfuryl alcohol due to the different characteristics of their physical properties, the location of the metal, and the metal-support interaction.

5.2 Recommendations

1. The further study the other factors such as temperature, H₂ pressure, and reaction time which effect on hydrogenation of furfural.
2. The study of another solvent in the hydrogenation of furfural which does not produce a solvent product and gives the desired product.

REFERENCES

- [1]. Bhogeswararao, S.; Srinivas, D., Catalytic conversion of furfural to industrial chemicals over supported Pt and Pd catalysts. *Journal of Catalysis* **2015**, *327*, 65-77.
- [2]. Merlo, A. B.; Vetere, V.; Ruggera, J. F.; Casella, M. L., Bimetallic PtSn catalyst for the selective hydrogenation of furfural to furfuryl alcohol in liquid-phase. *Catalysis Communications* **2009**, *10* (13), 1665-1669.
- [3]. Chen, X.; Zhang, L.; Zhang, B.; Guo, X.; Mu, X., Highly selective hydrogenation of furfural to furfuryl alcohol over Pt nanoparticles supported on g-C₃N₄ nanosheets catalysts in water. *Sci Rep* **2016**, *6*, 28558.
- [4]. Taylor, M. J.; Durndell, L. J.; Isaacs, M. A.; Parlett, C. M. A.; Wilson, K.; Lee, A. F.; Kyriakou, G., Highly selective hydrogenation of furfural over supported Pt nanoparticles under mild conditions. *Applied Catalysis B: Environmental* **2016**, *180*, 580-585.
- [5]. Liu, L.; Lou, H.; Chen, M., Selective hydrogenation of furfural over Pt based and Pd based bimetallic catalysts supported on modified multiwalled carbon nanotubes (MWNT). *Applied Catalysis A: General* **2018**, *550*, 1-10.
- [6]. Bagheri, S.; Muhd Julkapli, N.; Bee Abd Hamid, S., Titanium dioxide as a catalyst support in heterogeneous catalysis. *ScientificWorldJournal* **2014**, *2014*, 727496.
- [7]. Englisch, M.; Lercher, J.; Jentys, A., Structure Sensitivity of the Hydrogenation of Crotonaldehyde over Pt/SiO₂ and Pt/TiO₂. **1997**; Vol. 166.
- [8]. Walling, C.; Bollyky, L., Homogeneous Hydrogenation in the Absence of Transition-Metal Catalysts. *Journal of the American Chemical Society* **1964**, *86*, 3750.
- [9]. Rylander, P. N., Hydrogenation and Dehydrogenation. *Ullmann's Encyclopedia of Industrial Chemistry*, Wiley-VCH **2005**.
- [10]. Brown, J. M. A.; Ram, S. S. Catalytic Hydrogenation.
<http://www.chem.wisc.edu/areas/reich/chem547/2-redox%7B04%7D.htm>.
- [11]. Rylander, P. N., Platinum metals in catalytic hydrogenation.
- [12]. Kruachao, K., Synthesis of PtCo/TiO₂ catalysts by flame spray pyrolysis for selective hydrogenation of furfural to furfuryl alcohol. 2017.

- [13]. WHO Regional Office for Europe, Copenhagen, Denmark. Chapter 6.11 Platinum. *Air Quality Guidelines 2000*.
- [14]. Audi, G.; Bersillon, O.; Blachot, J.; Wapstra, A. H., The Nubase evaluation of nuclear and decay properties. *Nuclear Physics A* **2003**, *729* (1), 3-128.
- [15]. Hunt, L. B.; F.M.Lever, Availability of the Platinum Metals. *Platinum Metals Rev.* **1969**, *13*, 126-138.
- [16]. Platinum. <https://www.lookchem.com/Periodic-Table/Platinum/>.
- [17]. Titanium Dioxide.
https://pubchem.ncbi.nlm.nih.gov/compound/titanium_dioxide#section=Top.
- [18]. Dai, S.; Wu, Y.; Sakai, T.; Du, Z.; Sakai, H.; Abe, M., Preparation of Highly Crystalline TiO₂ Nanostructures by Acid-assisted Hydrothermal Treatment of Hexagonal-structured Nanocrystalline Titania/Cetyltrimethylammonium Bromide Nanoskeleton. *Nanoscale Res Lett* **2010**, *5* (11), 1829-1835.
- [19]. Davis, K. A., Titanium Dioxide. *Journal of Chemical Education* **1982**, *59*, 158.
- [20]. Su, C.; Hong, B.-Y.; Tseng, C.-M., Sol-gel preparation and photocatalysis of titanium dioxide. *Catalysis Today* **2004**, *96*, 119-126.
- [21]. Bashiri, R.; Mohamed, N. M.; Kait, C. F., Advancement of Sol-Gel-Prepared TiO₂ Photocatalyst. In *Recent Applications in Sol-Gel Synthesis*, 2017.
- [22]. Ullattil, S. G.; Periyat, P., Sol-Gel Synthesis of Titanium Dioxide. In *Sol-Gel Materials for Energy, Environment and Electronic Applications*, 2017; pp 271-283.
- [23]. Pan, C.-J.; Tsai, M.-C.; Su, W.-N.; Rick, J.; Akalework, N. G.; Agegnehu, A. K.; Cheng, S.-Y.; Hwang, B.-J., Tuning/exploiting Strong Metal-Support Interaction (SMSI) in Heterogeneous Catalysis. *Journal of the Taiwan Institute of Chemical Engineers* **2017**, *74*, 154-186.
- [24]. Tanabe, K., Application of niobium oxides as catalysts. *Catalysis Today* **1990**, *8*, 1-11.
- [25]. Tauster, S. J., Strong Metal-Support Interactions. Group 8 Noble Metals Supported on TiO₂. *Journal of the American Chemical Society* **1978**, *100*.
- [26]. Musci, J. J.; Merlo, A. B.; Casella, M. L., Aqueous phase hydrogenation of furfural

using carbon-supported Ru and RuSn catalysts. *Catalysis Today* **2017**, *296*, 43-50.

[27]. Zhang, C.; Lai, Q.; Holles, J. H., Bimetallic overlayer catalysts with high selectivity and reactivity for furfural hydrogenation. *Catalysis Communications* **2017**, *89*, 77-80.

[28]. Kijenski, J., Platinum deposited on monolayer supports in selective hydrogenation of furfural to furfuryl alcohol. *Applied Catalysis A: General* **2002**, *23*.

[29]. O'Driscoll, Á.; Curtin, T.; Hernández, W. Y.; Van Der Voort, P.; Leahy, J. J., Hydrogenation of Furfural with a Pt-Sn Catalyst: The Suitability to Sustainable Industrial Application. *Organic Process Research & Development* **2016**, *20* (11), 1917-1929.

[30]. Jiménez-Gómez, C. P.; Cecilia, J. A.; Moreno-Tost, R.; Maireles-Torres, P., Selective Furfural Hydrogenation to Furfuryl Alcohol Using Cu-Based Catalysts Supported on Clay Minerals. *Topics in Catalysis* **2017**, *60* (15-16), 1040-1053.

[31]. Salnikova, K.; Matveeva, V.; Bykov, A.; Demidenko, G.; Shkileva, I.; Sulman, E., The Liquid Phase Catalytic Hydrogenation of the Furfural *Chemical engineering transactions* **2018**, *70*.

[32]. Chen, B.; Li, F.; Huang, Z.; Yuan, G., Tuning catalytic selectivity of liquid-phase hydrogenation of furfural via synergistic effects of supported bimetallic catalysts. *Applied Catalysis A: General* **2015**, *500*, 23-29.

[33]. Li, Y.; Xu, B.; Fan, Y.; Feng, N.; Qiu, A.; He, J. M. J.; Yang, H.; Chen, Y., The effect of titania polymorph on the strong metal-support interaction of Pd/TiO₂ catalysts and their application in the liquid phase selective hydrogenation of long chain alkadienes. *Journal of Molecular Catalysis A: Chemical* **2004**, *216* (1), 107-114.

[34]. Ramprakash Upadhyay, P.; Srivastava, V., Selective Hydrogenation of CO to methane over TiO₂-supported Ruthenium nanoparticles. *Materials Today: Proceedings* **2016**, *3* (10), 4093-4096.

[35]. Chen, R.; Du, Y.; Xing, W.; Xu, N., The Effect of Titania Structure on Ni/TiO₂ Catalysts for p-Nitrophenol Hydrogenation. *Chinese Journal of Chemical Engineering* **2006**, *14* (5), 665-669.

[36]. Panpronot, J.; Kontapakdee, K.; Praserttham, P., Effect of TiO₂ Crystalline Phase Composition on the Physicochemical and Catalytic Properties of Pd/TiO₂ in Selective

Acetylene Hydrogenation. *J. Phys. chem* **2006**, *110*, 8019-8024.

- [37]. Chen, J.; Yao, N.; Wang, R.; Zhang, J., Hydrogenation of chloronitrobenzene to chloroaniline over Ni/TiO₂ catalysts prepared by sol-gel method. *Chemical engineering Journal* **2009**, *148*.
- [38]. Sikong, L.; Damchan, J.; Kooptarnond, K.; Niyomwas, S., Effect of doped SiO₂ and calcinations temperature on phase transformation of TiO₂ photocatalyst prepared by sol-gel method. *Songklanakarin J. Sci. Technol* **2008**, *30*.
- [39]. Yongjun Chen; Dionysiou, D. D., Effect of calcination temperature on the photocatalytic activity and adhesion of TiO₂ films prepared by the P-25 powder-modified sol-gel method. *Journal of Molecular Catalysis A: Chemical* **2006**, *244*.
- [40]. Wang, G.; Xu, D.; Guo, W.; Wei, X.; Sheng, Z.; Li, Z., Preparation of TiO₂ nanoparticle and photocatalytic properties on the degradation of phenol. *IOP Conference Series: Earth and Environmental Science* **2017**, *59*.
- [41]. Kuhaudomlap, S.; Mekasuwandumrong, O.; Praserttham, P.; Fujita, S.-I.; Arai, M.; Panpranot, J., The H₂-Treated TiO₂ Supported Pt Catalysts Prepared by Strong Electrostatic Adsorption for Liquid-Phase Selective Hydrogenation. *Catalysts* **2018**, *8* (2).
- [42]. Zhang, C.; He, H.; Tanaka, K.-i., Catalytic performance and mechanism of a Pt/TiO₂ catalyst for the oxidation of formaldehyde at room temperature. *Applied Catalysis B: Environmental* **2006**, *65* (1-2), 37-43.
- [43]. Ram, S., Ammonium Formate in Organic Synthesis. A Versatile Agent for Catalytic Hydrogen Transfer Reductions. *Synthesis* **1988**, *91*.
- [44]. Piyapaka, K.; Tungkamani, S.; Phongaksorn, M., Effect of Strong Metal Support Interactions of Supported Ni and Ni-Co Catalyst on Metal Dispersion and Catalytic Activity toward Dry Methane Reforming Reaction. *King Mongkut's University of Technology North Bangkok International Journal of Applied Science and Technology* **2016**.
- [45]. Pisduangdaw, S.; Mekasuwandumrong, O.; Yoshida, H.; Fujita, S.-I.; Arai, M.; Panpranot, J., Flame-made Pt/TiO₂ catalysts for the liquid-phase selective hydrogenation of 3-nitrostyrene. *Applied Catalysis A: General* **2015**, *490*, 193-200.
- [46]. J. Abad, C. Gonzalez, P.L. de Andres, and E. Roman, Characterization of silicon

thin overlayers on rutile TiO₂ (110)-(1x1). *Material Science* **2018**.

[47]. Pongthawornsakun, B.; Phatyenchuen, S.; Panpranot, J.; Praserttham, P., The low temperature selective oxidation of H₂S to elemental sulfur on TiO₂ supported V₂O₅ catalysts. *Journal of Environmental Chemical Engineering* **2018**, 6 (1), 1414-1423.

[48]. Hyung-Joo Choi, J.-S. K., Misook Kang, Photodecomposition of Concentrated Ammonia over Nanometer-sized TiO₂, V-TiO₂, and Pt/V-TiO₂ Photocatalysts. *Bull. Korean Chem. Soc.* **2007**, 28, 4.

[49]. Bharti, B.; Kumar, S.; Lee, H. N.; Kumar, R., Formation of oxygen vacancies and Ti³⁺ state in TiO₂ thin film and enhanced optical properties by air plasma treatment. *Sci Rep* **2016**, 6, 32355.

[50]. Yu, L.; Shao, Y.; Li, D., Direct combination of hydrogen evolution from water and methane conversion in a photocatalytic system over Pt/TiO₂. *Applied Catalysis B: Environmental* **2017**, 204, 216-223.

[51]. Islam, M. M.; Calatayud, M.; Pacchioni, G., Hydrogen Adsorption and Diffusion on the Anatase TiO₂(101) Surface: A First-Principles Investigation. *The Journal of Physical Chemistry C* **2011**, 115 (14), 6809-6814.

[52]. Durndell, L. J.; Parlett, C. M.; Hondow, N. S.; Isaacs, M. A.; Wilson, K.; Lee, A. F., Selectivity control in Pt-catalyzed cinnamaldehyde hydrogenation. *Sci Rep* **2015**, 5, 9425.

[53]. Di Paola, A.; Bellardita, M.; Palmisano, L., Brookite, the Least Known TiO₂ Photocatalyst. *Catalysts* **2013**, 3 (1), 36-73.

[54]. Zhang, Y.; Chen, L.; Mao, S.; Sun, Z.; Song, Y.; Zhao, R., Fabrication of porous graphene electrodes via CO₂ activation for the enhancement of capacitive deionization. *J Colloid Interface Sci* **2019**, 536, 252-260.

[55]. S. et.al, Classification of hysteresis loops. *Pure & Appl. Chem.* **1985**, 57, 603-619.

[56]. Venkatachalam, N.; Palanichamy, M.; Murugesan, V., Sol-gel preparation and characterization of nanosize TiO₂: Its photocatalytic performance. *Materials Chemistry and Physics* **2007**, 104 (2-3), 454-459.

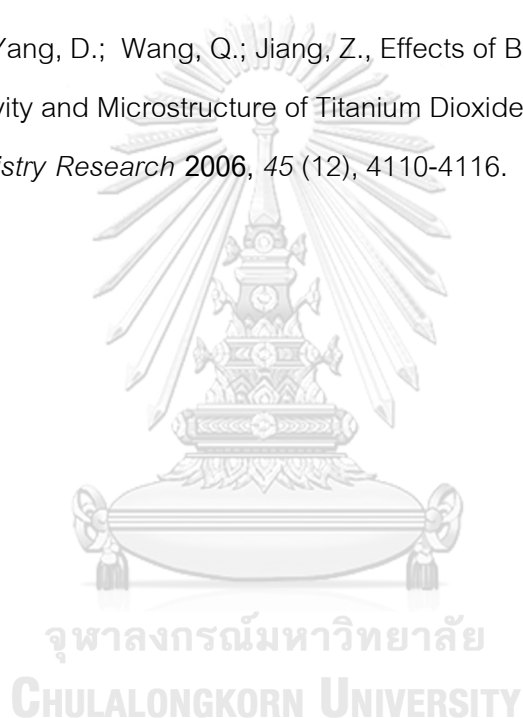
[57]. Dodoo-Arhin, D.; Buabeng, F. P.; Mwabora, J. M.; Amaniampong, P. N.; Agbe, H.; Nyankson, E.; Obada, D. O.; Asiedu, N. Y., The effect of titanium dioxide synthesis

technique and its photocatalytic degradation of organic dye pollutants. *Heliyon* **2018**, *4* (7), e00681.

[58]. Panpranot, J.; Kontapakdee, K.; Praserttham, P., Effect of TiO₂ Crystalline Phase Composition on the Physiochemical and Catalytic Properties of Pd/TiO₂ in Selective Acetylene Hydrogenation. *The Journal of Physical Chemistry B* **2006**, *110*.

[59]. Li, G.; Yao, S.; Zhu, J.; Liu, C.; Xing, W., The enhancement effect of nitrogen, fluorine-codoped titanium dioxide on the carbon supported platinum nano-catalyst for methanol electrooxidation reaction. *Journal of Power Sources* **2015**, *278*, 9-17.

[60]. Chen, D.; Yang, D.; Wang, Q.; Jiang, Z., Effects of Boron Doping on Photocatalytic Activity and Microstructure of Titanium Dioxide Nanoparticles. *Industrial & Engineering Chemistry Research* **2006**, *45* (12), 4110-4116.





APPENDIX

จุฬาลงกรณ์มหาวิทยาลัย
CHULALONGKORN UNIVERSITY

APPENDIX A

CALCULATION FOR CARALYST PREPARATION

For 0.5%Pt/TiO₂ catalysts prepared by incipient wetness impregnation method were shown below.

In this work, 1 g of the TiO₂ supports were used for all preparation and determined based on 100 g of catalysts used.

Reagents: Platinum (II)acetyl-acetonate 99.99%
Titanium (IV)butoxide reagent grade, 97%
Xylene 99.8%

Based on 1 g of catalysts used, the composition of catalysts will be as follows:

TiO₂ 100-0.5 = 99.5 g
Platinum 0.5 g
For TiO₂ 1 g
Platinum required = (1 g * 0.5 g)/100 = 0.005 g
TiO₂ required = 1-0.005 = 0.995 g

Platinum 0.005 g was prepared by using Platinum (II)acetyl-acetonate 99.99%

$$= \frac{\text{MW. of platinum (II) acetal-acetonate} * \text{weight of platinum required}}{\text{MW. of platinum}}$$

$$= \frac{323.29 \frac{\text{g}}{\text{mol}} * 0.005 \text{ g}}{195.078 \text{ /mol}}$$

$$= 0.0101 \text{ g.}$$

APPENDIX B
CALCULATION OF THE CRYSTALLITE SIZE

Calculation of the crystallite size by Debye-Scherrer equation

The crystallite size calculation from the width at half of height or full width of the diffraction peak of the XRD pattern using the Debye-Scherrer equation.

From Scherrer equation

$$D = \frac{\kappa\lambda}{\beta \cos\theta}$$

Where D = Crystallite size, Å

K = crystallite-shape factor = 0.9

λ = X-ray wavelength, 1.5418 Å for CuK α

θ = Observed peak angle, degree

β = X-ray diffraction broadening, radian

X-ray diffraction broadening (β) is the corrected width of a powder diffraction free from all broadening due to the instrument. The α -alumina was used as a standard sample to observe the instrumental broadening data. The most common correction for the X-ray diffraction broadening (β) can be obtained by

From Warren's formula:

$$\beta = \sqrt{B_m^2 - B_s^2}$$

Where B_M = The measured peak width in radians at half peak height

B_S = The corresponding width of the standard material

Example: Calculation of the crystallite size of anatase TiO₂ (A2)

The major peak of anatase TiO₂ was observed at $2\theta = 25.31^\circ$

The half-height width of the diffraction peak at $25.31^\circ = 0.30$

$$= \frac{2\pi \times 0.30}{360}$$

$$= 0.0052 \text{ radian}$$

Corresponding the half-height width of α -alumina of the diffraction peak at $25.31^\circ = 0.0041$ radian (BS)

$$\beta = \sqrt{B_m^2 - B_s^2}$$

$$= \sqrt{0.0052^2 - 0.0041^2}$$

$$= 0.0052 \text{ radian}$$

Thus,

$$K = 0.9$$

$$\lambda = 1.5418 \text{ \AA}^\circ \text{ for CuK}\alpha$$

$$\theta = 25.31/2 = 12.66$$

$$\beta = 0.0052 \text{ radian}$$

$$D = \frac{k\lambda}{\beta \cos \theta}$$

$$D = \frac{0.9 \times 1.5418}{0.0052 \times \cos 12.66}$$

$$D = 274 \text{ \AA}^\circ$$

$$D = 27.4 \text{ nm}$$

APPENDIX C

CALCULATION OF THE PHASE COMPOSITION

The fraction of crystal phase of TiO_2 was determined from X-ray diffraction. The phase composition of TiO_2 was calculated from:

$$W_R = \frac{1}{0.884 \times \frac{A}{R} + 1} \times 100$$

Where W_R = the percentage of rutile

A = the peak area of anatase TiO_2 at (101)

R = the peak area of rutile TiO_2 at (101)

The number of 0.884 is the coefficient of scattering

Example: Calculation of phase composition of TiO_2

From,

$$W_R = \frac{1}{0.884 \times \frac{A}{R} + 1} \times 100$$

$$W_R = \frac{1}{0.884 \times \frac{6599.38}{354.65} + 1} \times 100$$

$$W_R = 6\%$$

$$W_A = 94\%$$

APPENDIX D

CALCULATION FOR METAL ACTIVE SITES AND DISPERSION

Calculation of Pt active sites and Pt dispersion of the catalyst by CO-chemisorption is as follows:

$$\text{Volume of CO adsorption on catalyst, } V_{\text{ads}} = \frac{V_{\text{inj}}}{m} \times \sum_{i=1}^n \left(1 - \frac{A_i}{A_f} \right)$$

Where V_{inj} = volume injected, 0.02 cm^3

m = mass of catalyst used, g

A_i = area of peak i

A_f = area of last peak

Pt active sites

$$\text{Pt active site} = S_f \times \frac{V_{\text{ads}}}{V_g} \times N_A$$

Where S_f = stoichiometry factor, CO adsorbed on Pt, CO:Pt=1

V_{ads} = volume adsorbed

V_g = molar volume of gas at STP, $22414 \text{ cm}^3/\text{mol}$

N_A = Avogadro's number, 6.023×10^{23} molecules/mol

Metal dispersion

$$\text{Metal dispersion (\%)} = 100 \times \frac{\text{molecule of Pt loaded}}{\text{molecule of Pt from CO adsorption}}$$

$$\%D = S_f \times \frac{V_{\text{ads}}}{V_g} \times \frac{\text{MW}}{\%M} \times 100\% \times 100\%$$

Where S_f = stoichiometry factor, CO adsorbed on Pt, CO:Pt=1

V_{ads} = volume adsorbed

V_g = molar volume of gas at STP, 22414 cm³/mol

MW = molecular weight of the metal

%M = weight percent of the active metal

APPENDIX E

CALCULATION FOR CATALYTIC PERFORMANCE

Calculation of conversion and selectivity of the catalysts are shown in this below.

The calibration curve of furfural and furfuryl alcohol are shown in Figure E1-E2.

$$\% \text{Conversion} = \frac{\text{Mole (in)} - \text{Mole (out)}}{\text{Mole (in)}} \times 100$$

$$\% \text{Furfural conversion} = \frac{\text{Mole of furfural (in)} - \text{Mole of furfural (out)}}{\text{Mole of furfural (in)}} \times 100$$

$$\% \text{Selectivity} = \frac{\text{Mole of product}}{\text{Mole of convert reactant}} \times 100$$

$$\% \text{Furfuryl alcohol selectivity} = \frac{\text{Mole of furfuryl alcohol}}{\text{Mole of converted furfural}} \times 100$$

Reaction result from GC-FID, found that two peaks product consisted of furfuryl alcohol peak and solvent product peak. So solvent product selectivity calculation below equation

$$\% \text{Solvent product selectivity} = 100 - \% \text{Furfuryl alcohol selectivity}$$

$$\% \text{Yield} = \text{conversion} \times \text{selectivity}$$

$$\% \text{ Furfuryl alcohol Yield} = \text{Furfural conversion} \times \text{Furfuryl alcohol selectivity}$$

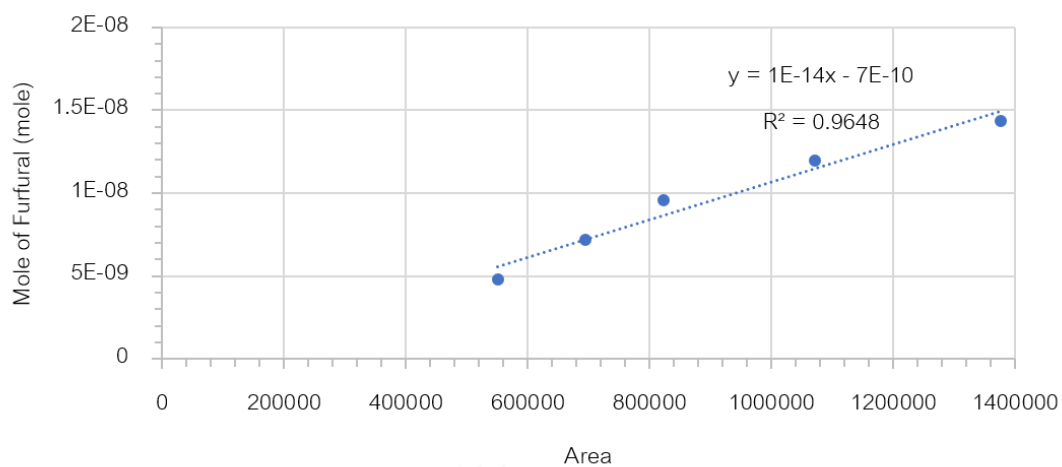


Figure E.1 The calibration curve of furfural

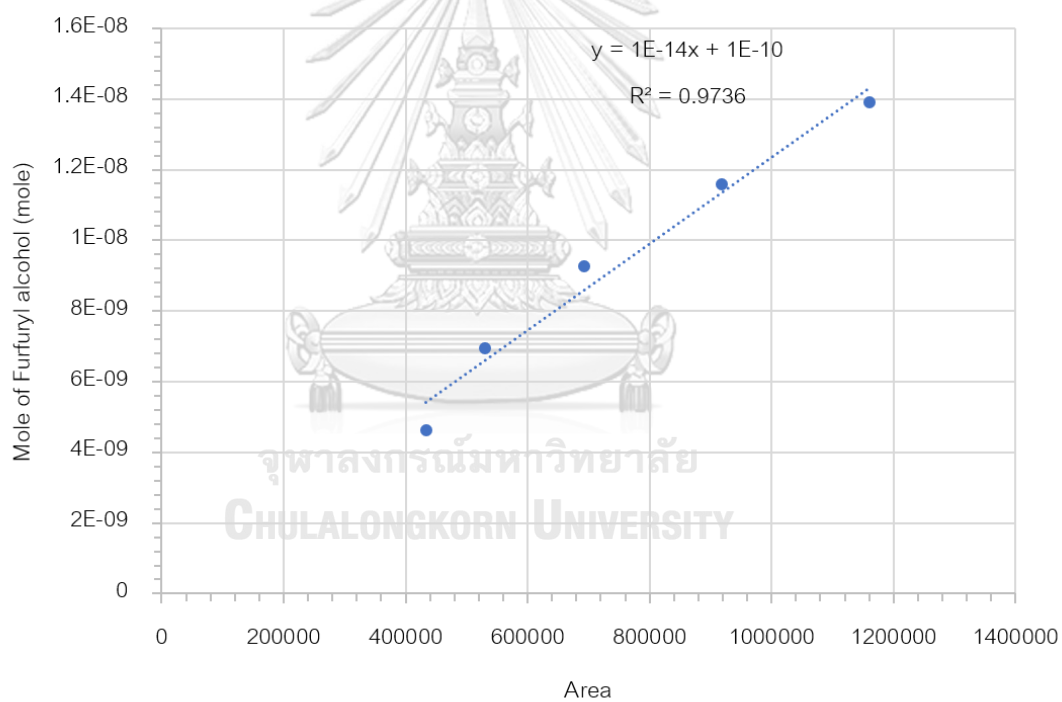


Figure E.2 The calibration curve of furfuryl alcohol

VITA

NAME Thunyaporn Kaewla-ueat

DATE OF BIRTH 31 October 1994

PLACE OF BIRTH Suratthani

INSTITUTIONS ATTENDED Bachelor Degree of Chemical Engineering from Faculty of Engineering, Prince of Songkla University, Thailand 2017.
She continued her Master study in the major in Chemical Engineering at Chulalongkorn University, Bangkok, Thailand in August 2017.

HOME ADDRESS 218/1 Moo 12 Na Tam Nuea, Amphone Muang Trang,
Trang, 92190